BNL-222653-2022-JAAM

Late day measurement of excised branches results in uncertainty in the estimation of two stomatal parameters derived from response curves in Populus deltoides Bartr. x Populus nigra L.

K. J. Davidson

To be published in "Tree Physiology"

January 2022

Environmental and Climate Sciences Department

Brookhaven National Laboratory

U.S. Department of Energy

USDOE Office of Science (SC), Biological and Environmental Research (BER) (SC-23)

Notice: This manuscript has been authored by employees of Brookhaven Science Associates, LLC under Contract No.DE-SC0012704 with the U.S. Department of Energy. The publisher by accepting the manuscript for publication acknowledges that the United States Government retains a non-exclusive, paid-up, irrevocable, world-wide license to publish or reproduce the published form of this manuscript, or allow others to do so, for United States Government purposes.

DISCLAIMER

This report was prepared as an account of work sponsored by an agency of the United States Government. Neither the United States Government nor any agency thereof, nor any of their employees, nor any of their contractors, subcontractors, or their employees, makes any warranty, express or implied, or assumes any legal liability or responsibility for the accuracy, completeness, or any third party's use or the results of such use of any information, apparatus, product, or process disclosed, or represents that its use would not infringe privately owned rights. Reference herein to any specific commercial product, process, or service by trade name, trademark, manufacturer, or otherwise, does not necessarily constitute or imply its endorsement, recommendation, or favoring by the United States Government or any agency thereof or its contractors or subcontractors. The views and opinions of authors expressed herein do not necessarily state or reflect those of the United States Government or any agency thereof.

Title: Late day measurement of excised branches results in uncertainty in the estimation of two stomatal parameters derived from response curves in *Populus deltoides* Bartr. x *Populus nigra* L.

Contributor Names: Kenneth J. Davidson[1,2], Julien Lamour[1], Alistair Rogers[1], Shawn P. Serbin[1]

Addresses for Contributors:

1. Department of Environmental and Climate Sciences, Brookhaven National Laboratory, Upton, NY, USA
2. Department of Ecology and Evolution, Stony Brook University, Stony Brook, NY, USA

Email address for author of correspondence: kdavidson@bnl.gov

Keywords: Stomata, Stomatal Response, Stomatal Optimality, Photosynthesis, Climate Model, Stomatal Conductance

Running head: Stomatal uncertainty due to excision and wait time

Abstract:

Many terrestrial biosphere models depend on an understanding of the relationship between stomatal conductance and photosynthesis. However, unlike the measurement of photosynthetic parameters, such as the maximum carboxylation capacity, where standard methods (e.g., CO_2 response or AC_i curves) are widely accepted, a consensus method for empirically measuring parameters representing stomatal response has not yet emerged. Most models of stomatal response to environment represent stomatal conductance as being bounded by a lower intercept parameter (g_0), and linearly scaled based on a multivariate term described by the stomatal slope parameter (g_1). Here we employ the widely used Unified Stomatal Optimization model, to test whether g_1 and g_0 parameters are impacted by the choice of measurement method, either on an intact branch, or a cut branch segment stored in water. We measured paired stomatal response curves on intact and excised branches of a hybrid poplar clone (*Populus deltoides* Bartr. x *Populus nigra* L. OP367), measured twice over a diurnal period. We found that predawn branch excision did not significantly affect measured g_0 and g_1 when measured within 4h of excision. Measurement in the afternoon resulted in significantly higher values of g_1 and lower values of g_0, with values changing by 55% and 56% respectively. Excision combined with afternoon measurement resulted in a marked effect on parameter estimates, with g_1 increasing 89% from morning to afternoon and a 25% lower g_1 for cut branches than those measured in situ. We also show that in hybrid poplar the differences in parameter estimates obtained from plants measured under different conditions can directly impact models of canopy function, reducing modelled transpiration by 18% over a simulated 12.5-hour period. While these results are only for a single isohydric woody species, our findings suggest that stomatal optimality parameters may not remain constant throughout the day.

Introduction:

Model representation of the exchange of carbon dioxide and water vapor between vegetative canopies and the atmosphere is a critical component of terrestrial biosphere models (TBMs). Both of these fluxes are fundamentally governed by stomatal control, which balances water loss through transpiration (E) against CO_2 entry into the leaf via photosynthesis (Hetherington and Woodward 2003). Many models of stomatal regulation assume that stomatal conductance (g_s), the rate of water vapor exiting leaf stomata, has evolved to be optimal with respect to water use, i.e. plants maximize carbon gain, per unit of water lost (Cowan and Fraquhar 1977; Damour et al. 2010). This optimal relationship can be represented empirically using the "Unified Stomatal Optimization" model (USO; Medlyn et al. 2011; Eqn. 1), which has two derived parameters, g_1 ($kPa^{0.5}$), typically referred to as the stomatal slope, which governs the relationship between the stomatal index (a multivariate term combining photosynthetic rate, CO_2 concentration, and leaf to air vapor pressure deficit) and g_s, and g_0 (mol m^2 s^{-1}) representing the expected stomatal conductance when net photosynthesis is zero. The model also has three measured variables, photosynthetic rate (A, µmol m^2 s^{-1}), the leaf to air vapor pressure deficit (D_s, kPa), and CO_2 concentration at the leaf surface (C_s, mol mol^{-1}). In the USO framework, g_1 is inversely proportional to water use efficiency, abbreviated WUE, and defined as $\partial E/\partial A$. A large g_1 is associated with a plant that loses more water per unit carbon assimilation than a plant with a low g_1.

Equation 1. $$g_s = g_0 + 1.6\left(1 + \frac{g_1}{\sqrt{D_s}}\right)\frac{A}{C_s}$$

Despite the fact that A and g_s rates directly impact global carbon and water cycles, their relationship continues to be a large source of variation in current model predictions (Ricciuto et

al. 2018). For example, Dietze *et al.* (2014) found that when unconstrained by data, g_1 was the second largest uncertainty in their analysis of global controls on net primary productivity. However, unlike many other photosynthetic parameters that can be derived from gas exchange measurements, no consensus exists on a standard method for estimating g_0 and g_1 (Bernacchi et al. 2013; Sharkey et al. 2007). One common method for assessing stomatal function is a survey-based approach, where rates of A and g_s are measured instantaneously under natural conditions, and g_1 and g_0 are fit from the data with regression analysis (e.g., Lin et al. 2015). Alternatively, many investigators have used a response curve approach for the estimation of stomatal behavior, in which the environment around a leaf (e.g., irradiance, atmospheric CO_2 concentration (C_a), or vapor pressure deficit (D or VPD)) is altered, and the operator observes how rates of steady state A and g_s respond (Ball et al. 1987; Leakey et al. 2006; Mott 1988). Unlike survey methods, response curves control for leaf-to-leaf variation in response, and capture a parameter estimate at a fixed point in time, and thus are an appealing method for fitting parameter estimates used in TBMs of vegetation function.

However, stomatal response curves are not without drawbacks, sometimes taking up to a full day to complete for a single leaf (Leakey et al. 2006). This poses a challenge when the species of interest is difficult to access, and for this reason, researchers often sample branches and conduct response curves ex situ, utilizing methods such as shotgun sampling (Serbin et al. 2014; Burnett et al. 2019; 2021), or manual branch pruning (Wu et al. 2019). However, with these ex situ measurements comes the assumption that excision of a branch will not fundamentally alter the response of the parameter of interest, through branch cavitation or other stress responses (Santiago and Mulkey 2003, Verryckt et al. 2020, Missik et al. 2021).

89 It is well known that excision can alter wood conduit structure by introducing air into the
90 xylem, which can lead to cavitation and embolism of tissue upstream of the cut (Williamson and
91 Milburn 1995). Xylem damage can also reduce the volume of water reaching the leaf tissue,
92 altering capacitance (Sperry et al. 1993), potentially influencing the relationship between A and g_s.
93 A number of studies (e.g., Verryckt et al. 2020, Santiago and Mulkey 2003, Missik et al. 2021,
94 Akalusi et al. 2021) have shown that if branches are immediately recut under water after initial
95 excision, rates of A and g_s may be unaffected. Importantly, however, these studies do not assess
96 changes in the parameters g_1 and g_0, stomatal traits which may be more acutely affected by
97 hydraulic damage if water supply to the leaf is impaired.
98 A final implicit assumption with the response curve approach is that the measured parameter
99 will be temporally constant, and thus will not change over the length of the measurement. In most
100 cases however, there is a contrast between the apparent parameter measured, and the ideal or
101 nominal value for the parameter. For example it is known that the maximum rate of Rubisco
102 carboxylation ($V_{cmax.25}$) declines over a diurnal time-course due to Rubisco deactivation, leading
103 late day estimation of $V_{cmax.25}$ to be up to 50% lower than the morning value (Salvucci and
104 Anderson 1987; Kobza and Seemann 1989). In addition, Resco de Dios *et al.* (2020) found that
105 changes in the circadian timing of metabolism over diurnal timescales leads to different "optimal"
106 levels of g_s, showing that assuming a fixed optimal level for stomatal parameters is not consistent
107 with observation.
108 Here we attempt to test two key assumptions of stomatal response curves in a controlled
109 manner, namely that time since branch excision, and the time of day in which a measurement is
110 made will not impact fitted parameter estimates. Our objective was to determine if g_1 and g_0
111 estimations were different between pairs of cut and intact branches, measured across two periods

during a day. Our specific research questions were; (1) does predawn excision of branches lead to a modified stomatal response to irradiance, compared with the intact in situ measurement curves? (2) Is g_1 diurnally dynamic, leading to shifts in WUE over the course of the day? (3) Will use of g_0 and g_1 estimated from excised or late day measurements produce different estimates of leaf scale transpiration?

Materials and Methods:

Plant material:

In May 2019, 20 cm hardwood stem cuttings of *Populus deltoides* Bartr. x *Populus nigra* L. OP367 (hybrid poplar) were soaked in water until roots formed and transplanted into 210 L pots filled with Pro-Mix M (Premier Tech, Quebec, Canada) potting soil. Plants were grown outside on a fenced concrete pad at Brookhaven National Laboratory (Upton, NY, USA, latitude: 40.8834319, longitude: -72.870103, elevation: 18 m above sea level). Mean annual temperature at the site is 10.3ºC, and mean annual precipitation is 1244.6 mm. During the period of study average temperature was 22.3ºC, and the site received a total of 114.3 mm of precipitation. Data collection took place during the second year of growth. During spring and summer, pots were irrigated every other day to field capacity to prevent soil from drying to the point at which the plants would experience soil water stress. During this period, three fertilizer treatments of Peters Professional 15-16-17 (ICL Specialty Fertilizers, Dublin, Ohio, USA) were applied, the last of which occurred seven days before the first measurements were taken. At each application, approximately 4.5 L of fertilizer mix was injected into the soil using a Dosatron D14MZ10 Fertilizer Injector (Dosatron International Inc., Clearwater, FL, USA), set to a mix rate of 200 ppm with the injector set at a 1:100 ratio fertilizer to water.

Measurements took place from July 15 - August 21, 2020. For each measurement day two plants were selected, and on each plant two equivalent branches were identified, one which would be excised predawn and the other to serve as an intact control. Prior to excision, a target leaf was identified and flagged on each of the four candidate branches. The target leaves were matched so that within each plant, leaves were of the same approximate size, color, phenological stage, and leaf plastochron index (LPI) (Erickson and Michelini 1957; Meicenheimer 2014; Rogers et al. 2012), a measure of the approximate age of a leaf based on its proximity to the most distal leaf which has expanded beyond 10 mm in length from base to apex. While the plant-to-plant criteria for leaf selection varied, the target leaves were always the most recently fully expanded, physiologically mature, and undamaged leaves. LPI ranged from 8-15, indicating that all leaves were physiologically mature and fully expanded. In this way, although the total plant to plant variation in target leaves was considerable, within each plant the target leaves were as closely matched as possible.

Predawn (approximately 30 minutes prior to nautical twilight) on the day of each measurement, two approximately 2.5 m candidate branches were cut for each of two plants. These branches would serve as the cut treatment for both the morning (AM) and afternoon (PM) measurement period. Each branch segment was then placed in a bucket containing 22 L of water, and immediately recut under water to prevent cavitation or embolism of the xylem (Wheeler et al. 2013, Sperry 2013). This method serves to remove embolized tissue, and allows for xylem tension to be relieved by drawing liquid water into the cut, thereby restoring the hydraulic driving gradient within the branch (Venturas et al. 2015). Each recut consisted of removing at least 50 cm of material to provide a sufficient buffer between the site of the second cut and any embolized xylem (Wolfe et al. 2016). After branches had been recut, they measured approximately 2 m in length.

We chose to make our initial branch cuts predawn as that is when water potential is closest to zero, no photosynthesis is occurring, ambient temperatures were low, and the branches and the intact plants were experiencing no thermal stress.

Cut branches were stored under ambient metrological conditions adjacent to their parent individual from the time of cutting until gas exchange measurement commenced. After gas exchange the four measured leaves were sampled for fresh mass and area. Fresh mass was taken on an ER-60A digital balance (A&D Weighing San Jose, CA, USA) and area was calculated from digital photographs with a scale reference and subsequently post processed using the software application ImageJ (v1.53a, National Institutes of Health, Bethesda, MD, USA). Dry mass was recorded after samples were dried to constant mass at 60°C. Leaf mass per area (LMA) was calculated as dry mass divided by the total leaf area. In total 32 curves were conducted (16 pairs).

Gas exchange measurements

All gas exchange measurements were conducted using one of two LI-6800 portable photosynthesis systems (LI-COR Inc., Lincoln, NE, USA) with either a Multiphase Flash Fluorometer leaf chamber (6800-01A) (first 16 curves) or a "Small Light Source" leaf chamber (6800-02) for the remaining curves. We found no significant effect of chamber type on either g_0 or g_1 estimates. For all measurements, the color spectrum of the irradiance was 90% red, 10% blue. Both LI-6800s were factory calibrated by the manufacturer three months prior to use and were running the same version of the operating system (v 1.14.05).

Stomatal response curves followed previously established methods (Leakey et al. 2006) in which irradiance was systematically adjusted in order to propagate changes in *A*, while holding VPD_{leaf} and sample CO_2 concentration (CO_2S) constant (Fig. 1). Before beginning the collection

of all experimental stomatal response curves, 10 irradiance response curves were conducted on randomly selected individuals at a leaf temperature of 30°C to determine the overall response of *A* to various levels of irradiance. From these curves, the response of *A* to irradiance was subdivided into 10 approximately equal levels representing the full range of irradiance and their corresponding levels of *A*, ranging from light saturated photosynthesis (A_{sat}), to respiratory CO_2 release in the dark (R_{dark}). The final irradiance levels chosen were as follows (1500, 900, 700, 450, 250, 175, 90, 40, 20, 0 μmol m^{-2} s^{-1}). We chose to decrease irradiance on a sun adapted leaf, rather than increase irradiance for a dark-adapted leaf as in general, stomata are known to react more slowly to increases in irradiance than decreases in irradiance (Lawson and Blatt 2014, Lawson and Vialet-Chabrand 2019), presumably as a mechanism to maximize carbon gain in unstable conditions (Lawson et al. 2012, Drake et al. 2013, McAusland et al. 2016). Thus, by conducting our response curves by decreasing irradiance, we estimate that the length of a single curve was reduced by approximately half. While the direction of a change in irradiance (increase vs decrease) does impact instantaneous water use efficiency (iWUE; A_n g_s^{-1}) immediately following the change in irradiance, this will have no impact on the steady state levels of *A* and g_s required to estimate g_1 and g_0.

Before the collection of each individual g_s response curve, a leaf temperature and VPD_{leaf} level was chosen that would be representative of the mean external environment for that day for the full length of the curve. As each curve took 5-6 hours to complete, leaf temperature set-point values often had to be higher than ambient air temperature in the morning to prevent reaching the dew point temperature later in the day when cooling was necessary. On average for the morning curves, T_{leaf} was 28.1ºC and VPD_{leaf} was 1.15 kPa. For the afternoon curves, mean T_{leaf} was 30.2ºC and mean VPD_{leaf} was 1.25 kPa. CO_2S was set to 400 μmol CO_2 mol^{-1} so that the level of CO_2 at the

leaf surface was approximately equivalent to the level of CO_2 outside the leaf chamber. CO_2S, VPD_{leaf}, and T_{leaf} were held constant for the entirety of each curve so that *A* and g_s response between curves were comparable and related only to the leaf-to-leaf variation at a given irradiance level on the experimental plants. An automatic logging program was used to collect a data point every 10 seconds for the duration of measurements, and the devices were set to automatically match sample and reference gas analyzers every 10 minutes.

Each curve began at 1500 PPFD. After a 1-hour acclimation and stabilization period, PPFD was dropped to the next lowest irradiance level, and leaves were allowed to acclimate to this new irradiance level for a minimum of 25 minutes. After the 25-minute acclimation period, *A* and g_s levels were monitored for stability in both leaves, after which the process was repeated until measurements at all 10 irradiance levels had been completed. For each irradiance level an average of the 5 log points prior to a change in irradiance constituted that measurement. Irradiance level was dropped for both branches simultaneously so that any external influences of ambient irradiance or wind on the curves would be equivalent between branches. Overall, both branches responded similarly to changes in irradiance, with negligible differences in stabilization times between treatments. Two pairs of curves were conducted per day, the morning treatment (~07:30-13:30 EST, hereafter AM treatment) and the afternoon treatment (~13:30-18:30 EST, hereafter PM treatment).

Estimation of stomatal conductance parameters

Stomatal response was evaluated using the USO model (Medlyn et al. 2011) (Equation 1). Using the USO model, data can be fit to estimate the two main parameters, a stomatal slope (g_1)

and an intercept (g_0). The g_0 parameter represents the expected g_s when A_{net}=0, which will occur at a PPFD equivalent to the light compensation point. The g_1 parameter represents the slope of the relationship between g_s and a combined term including C_s, D_s, and A, sometimes termed the stomatal index. It should be noted that while Equation 1 uses the term C_s, C_a is often used in its place when data are derived using gas exchange systems, as the two values are identical when the effect of boundary layer conductance is eliminated.

Equation 1 can be rewritten as a linear model where g_1 is the slope term, and g_0 is the intercept term, as in other Ball-Berry type model formulations (e.g., Ball et al. 1987, Leuning 1995, Katul et al. 2010; Equation 2; Fig. 1b). g_1 and g_0 are mathematically identical in Equation 1 and 2, however Equation 2 provides for simpler graphical depiction of the data and will be used throughout.

Equation 2. $$g_s - \frac{1.6A}{C_s} = g_0 + g_1 * \left(\frac{1.6A}{C_s\sqrt{D_s}}\right)$$

Typically, the model parameters g_0 and g_1 are simultaneously fitted so that the model best represents the observations. However, several authors have shown a strong correlation between the estimates of g_0 and g_1 which can lead to interdependency in their estimation (Damour et al. 2010; Duursma et al. 2019), which can bias estimates of g_1 based on g_0. Alternatively, other authors (e.g., Leuning 1995) have suggested to use another method where g_0 is fixed either as 0, or as a given positive value to minimize the impact of g_0 on g_1 estimation. To account for this concern, we used two approaches to fit g_0 and g_1. In the first approach, both g_0 and g_1 are simultaneously estimated for each treatment group, and both g_0 and g_1 are reported. In the second approach, a population value for g_0 was estimated by extrapolating g_s at a value of A_n = 0 from points just above and below the light compensation point for each curve, then taking the mean of these values for the full population of curves (hereafter $g_{0,population}$; 0.037 mol m^{-2} s^{-1}). Then, using $g_{0,population}$ as the

intercept, g_1 was estimated for each treatment group. For models which use $g_{0,population}$ as the intercept, only the g_1 value is reported.

Leaf biochemical analysis for modeling synthesis

To estimate V_{cmax} we used the "one-point method" (De Kauwe et al. 2016, Equation 3), which has shown comparable results to traditional AC_i curves in this species (Burnett et al. 2019):

Equation 3. $$V_{cmax} = \frac{A_{sat}}{\left(\frac{C_i - \Gamma^*}{C_i + K_m} - 0.015\right)}$$

where K_m is the Michaelis–Menten constant (404.9 µmol mol^{-1}), Γ* is the CO_2 compensation point in the absence of mitochondrial respiration, and C_i is the intercellular CO_2 concentration.

The "one-point" data used were our first point on each stomatal response curve, as it was an acclimated, steady state, light saturated measurement at 400 ppm CO_2. V_{cmax} at measurement temperature was then scaled to V_{cmax} at 25°C using a modified Arrhenius equation (Leuning 2002, Equation 4) with the kinetic constants provided in Bernacchi et al. 2001):

Equation 4. $$V_{cmax.25} = \frac{C * \exp\left[(H_a / RT_{25})(1 - T_{25}/T_{leaf})\right]}{1 + \exp\left[(S_V T_{leaf} - H_d)/(RT_{leaf})\right]}$$

where $V_{cmax.25}$ is the value of V_{cmax} at the reference temperature (T_{25} = 298.15 K), $V_{cmax.T}$ is the value of V_{cmax} at the leaf temperature (T_{leaf} in K), H_a, H_d, and S_v are the activation and deactivation energies of the enzyme Rubisco and an entropy term (H_a = 65330 J mol^{-1}, H_d =149250 J mol^{-1}, S_v = 486 J mol^{-1} K^{-1}), R is the ideal gas constant (R = 8.314 J mol^{-1} K^{-1}), and C is a combined term equivalent to $1 + \exp[(S_v T_{25} - H_d)/(RT_{25})]$.

J_{max} at 25°C was then calculated as 1.615 * $V_{cmax.25}$, a ratio observed in values collected from AC_i curves in a previous study on the same individuals (Walker et al. 2021). $R_{dark.T}$ was calculated from dark adapted measurements of A (the final response curve point) and was scaled to 25°C

($R_{dark.25}$) using an inverse Arrhenius equation (Equation 5; Bernacchi et al. 2001, Von Caemmerer 2013):

Equation 5. $$R_{dark.25} = \frac{R_{dark.T}}{\exp\left(\frac{H_a}{(R*T_{25})} - \frac{H_a}{(R*T_{leaf})}\right)}$$

where H_a is the activation energy of mitochondrial respiration (H_a = 46390 J mol^{-1}).

Statistical analysis

To test the effect of branch excision and time of day on g_0 and g_1 we used a mixed effect model, with two fixed effects: excision (cut and intact) and the time of day (AM and PM). We also tested the interaction between these two factors. We have a total of 32 curves (8 cut-AM, 8 intact-AM, 8 cut-PM, 8 intact-PM), each consisting of 10 points for 320 total measurements. However, points within each curve are non-independent, making this an excellent application for mixed models, with leaf considered as a random effect on g_0 and g_1. We also used mixed models to test for an effect of LMA and fresh mass on g_0 and g_1. In all mixed models, we consider a $p < 0.05$ as evidence of a significant result, and the differences between group means were assessed using a post hoc Tukey's HSD test (Tukey 1949).

Paired sample t-tests were used to compare cut and intact LMA, fresh mass, V_{cmax}, A and C_i. Paired sample t-tests were also used to examine the effect of time of day on the same leaf properties. To examine the effect of leaf on stomatal traits, we constructed linear models of LMA, fresh mass: dry mass, V_{cmax}, and R_{dark} versus g_0 and g_1. Models with a slope not significantly different from 0 were considered to be non-significant.

All analyses were performed using the software package R (v 3.6.2, R Core Team 2013); mixed models were constructed and tested using the package 'nlme' (v 3.1, Pinheiro et al. 2020) and contrast estimates were analyzed with the package 'emmeans' (v 1.4.8 Lenth et al. 2020).

Leaf Gas exchange simulation

In order to simulate A and g_s in response to ambient environmental conditions, we used a coupled leaf scale steady state assimilation, conductance, and energy balance model included in the R package 'LeafGasExchange' (v 1.0.1 Lamour and Serbin 2021). The model first simulates environmental conditions at the leaf surface. It uses meteorological data for the study site obtained from the Brookhaven National Lab Meteorological Service (https://www.bnl.gov/weather/), which records air temperature, wind speed, irradiance level, and atmospheric pressure at one-minute time intervals.

We use a leaf energy budget model published by Muir (2019, 2020) to simulate T_{leaf}, C_s, and VPD_{leaf}. This energy budget uses an iterative solving function to estimate T_{leaf} and boundary layer conductance (g_{bw}) by first assuming $T_{leaf} = T_{air} + 1$ºC, $C_s = C_a$, and $VPD_{leaf} = VPD_{air}$, then solving for A, g_s, C_i, $T_{leaf,}$ and g_{bw} accounting for the temperature dependencies of the photosynthetic parameters $R_{dark,}$ V_{cmax}, and J_{max} (Bernacchi et al. 2001, Leuning 2002, Bernacchi et al. 2003b, Von Caemmerer 2013). Then the model compares the resulting estimation of T_{leaf} to the prior value, and if the values are within 0.1°C, assumes the model has converged. If the values differ by more than 0.1°C, the model is rerun using the updated values of Tleaf, C_s, and VPD_{leaf}.

Stomatal conductance is simulated using the USO model (Medlyn et al. 2011) shown in Equation 1. Photosynthesis is simulated using the FvCB assimilation model (Farquhar et al. 1980) which assumes that net photosynthesis (A_n) is the minimum of carboxylation limited assimilation (A_c) and RuBp regeneration limited assimilation (A_j), minus the respiration rate that is not attributable to the photorespiratory pathway (R_{dark}). The model uses parameters for the maximum rate of electron transport at 25°C ($J_{max.25}$), maximum rate of carboxylation at 25°C ($V_{cmax.25}$), and

the leaf dark respiration rate at 25°C ($R_{dark.25}$) which are scaled to T_{leaf} using an Arrhenius function or an inverse Arrhenius function (Bernacchi et al. 2001, 2003b, Leuning 2002, Von Caemmerer 2013). The model was parameterised using $V_{cmax.25}$, $J_{max.25}$, $R_{dark.25}$, g_0, and g_1 calibrated using the data from this study. For the other parameters necessary to calculate photosynthesis, default parameters for C_3 plant species were chosen (Lamour and Serbin 2021; Table S1). For all model simulations, uncertainty was modeled by rerunning the model using g_1 and g_0 values corresponding to ± SE of the fitted value.

Two different types of models were run using these data, one run simulating A and g_s over a 12-hour time period on each day of data collection, and one using an "average day" which was an aggregation of the mean daytime metrological parameters at one-minute intervals. We also ran the model across an expected range in leaf temperature, VPD_{leaf}, and irradiance to ensure changes in A, g_s, and C_i were as expected (Fig. S1)

Results:

Stomatal Model Parameters:

When looking at the overall effect of time of day on stomatal parameters we find a significant increase ($F_{2,298}$ = 126.6, p< 0.001) in g_1 by 55% between the AM and PM treatment, and a significant ($F_{2,298}$ = 20.2, p< 0.001) 56% decrease in g_0 between AM and PM treatments. When using $g_{0,population}$ in place of g_0, there was a significant ($F_{2,298}$ = 68.0, p< 0.001) 89% increase in g_1 from AM to PM, a larger effect than seen with the model which considers both g_0 and g_1 (Table 1, Fig. 2b-c).

Next, when considering the interaction of excision and time of day we find a significant effect on g_1 ($F_{4,294}$ = 64.3, p< 0.001), g_0 ($F_{4,294}$ = 17.1, p< 0.001), and g_1 when using $g_{0,population}$ ($F_{4,298}$ =

68.0, p< 0.001; Table 2). The parameter g_1 increased by 49% between AM and PM in the cut treatment (t_{296} = -2.7, p = 0.0334) whereas it only increased by 36% for the intact treatment (t_{296} = -3.5, p = 0.0036, Fig. 3c-d). The g_0 parameter followed a similar pattern, with a 66% decrease between AM-cut and PM-cut treatments (t_{296} = 3.9, p < 0.001), however there was no significant difference between AM and PM in the intact treatment (Table 2, Fig. 3a-b). When $g_{0,population}$ was used, all pairwise comparisons of g_1 were significant, except the comparison between AM-cut and AM-intact treatments (Table 2, Fig. 3e-f). Across all significant contrast, g_1 was lower in the AM treatment than the PM treatment and lower for the cut treatment than the intact treatment (Fig. 2c).

Finally, we observed a significant ($F_{2,298}$ = 71.0, p< 0.001) 9% reduction in g_1 measured on leaves from excised branches respective to leaves from intact branches, and a smaller significant ($F_{2,298}$= 51.7, p<0.001) 6% reduction in g_0. When using $g_{0,population}$ in place of g_0 we observed a significant ($F_{2,300}$= 102.2, p<0.001) 10% reduction in g_1 for the cut treatment over the intact treatment (Table 1, Fig. 2a). However, these effects of excision are likely due to large differences in treatments in the PM group, as we find no significant differences between AM-cut and AM-intact treatments.

Leaf Traits

Paired sample t-tests revealed no significant (p < 0.05) difference in leaf traits (LMA, mass:dry mass ratio, $R_{dark.25}$, $V_{cmax.25}$) between cut and intact leaves or leaves from the AM and PM treatments, aside from a significant ($t_{21.58}$ = -2.23, p = 0.037) 29.7% increase in $V_{cmax.25}$ from AM to PM (Fig. 4a-d). A full list of treatment level leaf trait means, and standard deviations, can be found in Table S2.

Differences in leaf structural properties had no significant effect on either g_1 or g_0 parameter estimates (Table S3). Both LMA and the ratio of fresh mass to dry mass show no significant relationship with fitted values of g_0 and g_1, suggesting that leaf to leaf variation in these properties was not a cause of other fixed effects trends in g_1 or g_0 (Fig. 4e-h).

Simulation of leaf level *A*, g_s, and *E*

Simulations using our coupled leaf assimilation, stomatal conductance, and energy balance model revealed stark differences in both the shape and overall magnitude of the leaf level *A* and *E* response (Fig. 5). Parametrization has a strong effect on the integrated daily level of *E*, with 2.73 ± 0.4 L m^{-2} for the AM-cut treatment, 2.76 ± 0.4 L m^{-2} for the AM-intact treatment, 3.04 ± 0.3 L m^{-2} for the PM-cut treatment, and 3.32 ± 0.36 L m^{-2} for the PM-intact treatment (Fig. 5c). Rates of daily integrated *A* followed a similar pattern with 0.390 ± 0.000039 kg m^{-2} for the AM-cut treatment, 0.387 ± 0.000039 kg m^{-2} for the AM-intact treatment, 0.391 ± 0.00039 kg m^{-2} for the PM-cut treatment, and 0.394 ± 0.00040 kg m^{-2} for the PM-intact treatment (Fig. 5d). We also see that when we compare a model which has fixed values of g_1, g_0, $V_{cmax.25}$, $J_{max.25}$, and $R_{dark.25}$, and a model where these values are dynamic with time of day (AM group values used from 06:00-13:00 and PM group values used from 13:01-18:30), the dynamic model produces estimates of *E* and *A* that are 8.6% and 1.1% respectively lower than the model which assumes fixed values.

Discussion:

Here we demonstrate that predawn excision, combined with late day measurement, can strongly influence parameter estimates of g_0 and g_1 in hybrid poplar. We see that in our PM

386 treatment, excision of a branch leads to a 25% lower g_1 estimate than in an intact control,
387 suggesting that WUE may increase as the result of branch excision. However, if measurements
388 were made within four hours of branch excision, we observed no significant difference in measured
389 g_0 or g_1. We also see that over the diurnal course g_0 decreases by 55% and g_1 increases by 56%,
390 irrespective of treatment. These differences mean that if PM-cut branches are used to derive values
391 of g_1 for models of intact branches, this can result in up to a 34% overestimation of leaf level g_s
392 for AM and mid-day periods. If extended over the course of a full day, the differences in estimated
393 g_1 between PM-intact and AM-cut branches led to a modeled level of transpiration that is 18%
394 higher than would be simulated when using AM-cut measurements alone.
395
396 Excision effect on g_1 and g_0:
397 When looking at excision alone as a factor influencing parameter estimates, there was only a
398 small effect of excision on branches, leading to a 10% reduction in g_1 for the cut treatment when
399 compared with the intact treatment. However, when the interaction of excision and time of day are
400 considered together, an important trend immerges. In the morning, g_1 was not significantly
401 different between the cut an intact treatment, however in the afternoon g_1 was 25% lower in the
402 cut treatment than the intact treatment (Fig. 3e-f). This finding, that there is no effect of excision
403 on g_1 when measurements are within four hours of branch removal, is critical as it reinforces the
404 validity of using ex situ measurements of excised branches for physiological study (Leakey et al.
405 2006, Verryckt et al. 2020, Missik et al. 2021). This observation also highlights that while excision
406 does not impact g_1 early in the day, over time the effect of excision becomes more pronounced.
407 This is, to our knowledge, the first study which directly compares the stomatal property g_1
408 between cut and intact branches, as typically one measurement method is chosen without any cross

409 comparison on the effect excision has on rates of A or g_s. While other studies have examined
410 excision effects (Santiago and Mulkey 2003, Leakey et al. 2006, Verryckt et al. 2020, Missik et
411 al. 2021) none have addressed the potential effects of excision on the stomatal parameter g_1 or g_0.
412 Missik et al., (2021) investigates rates of A and g_s relative to time since excision, finding that for
413 the three species studied, rates of A decline by between 25-63%, and rates of g_s decline by 31-43%.
414 Missik and colleagues (2021) also examine the literature for similar studies, finding that of 13
415 previous studies which examine excised branches, only one examines a quantitative difference in
416 rates of A and g_s. That study (Santiago and Mulkey 2003) examines the impact of excision on both
417 sustained rates of A and on photosynthetic response curves in 10 tropical canopy tree species.
418 Santiago and Mulkey (2003) suggest that an excision induced decline in g_s may be the cause of
419 their observed decline in A, however they lack strong evidence for this claim. Leakey et al., (2006)
420 measured rates of A and g_s in excised leaves of soybean (*Glycine max* [L.]) in order to parametrize
421 a model of crop photosynthesis and transpiration. Leakey and colleagues, (2006) then tested the
422 parametrization of these laboratory derived data by comparing measured and modeled rates of g_s
423 finding that they were highly correlated, with a non-significant bias. Finally, Verryckt et al., (2020)
424 explores the effect of excision on rates of A in tropical species. However they do not examine any
425 impact of excision on rates of g_s, limiting the comparisons that can be drawn between their work
426 and this study.

427 In addition to the effect of excision on g_1 we also observe a difference in g_0 between treatments,
428 with g_0 being slightly (6%) lower for the cut group than the intact group. This finding, that g_0 is
429 lower for the cut treatment, aligns well with existing stomatal (Cowan and Fraquhar 1977) and
430 hydraulic (Katul et al. 2003) optimality frameworks, which suggest that a lower g_0 is a more water
431 use efficient behavior, as any g_s at values of $A_{net} \leq 0$ is water "wasted" with no net photosynthetic

gain, unless as offsetting thermal stress alone (Cowan 1978; Cowan and Fraquhar 1977, Blackman et al. 2016, Miner et al. 2017, Martin-StPaul et al. 2017). While it is not biologically possible for g_s to be exactly equal to 0 due to cuticular leakage and incomplete stomatal closure (Duursma et al. 2019) lower g_0 is commonly associated with species in arid regions where any loss of water with no gain in carbon is maladaptive (Duursma et al. 2019; Kerstiens 1996; Machado et al. 2021; Martin-StPaul et al. 2017). Based on this reasoning, we expected a decrease in g_1 to be accompanied with a concurrent drop in g_0. However, we did not observe this pattern in any of our comparisons. This unexpected finding may be because the hybrid poplar we used in this study is an agricultural variety, bread for fast biomass accumulation, and thus its stomatal dynamics may not be adapted for maximum water retention at low irradiance.

Time of day effect on g_1 and g_0:

In their optimization model of stomatal function, Cowan and Fraquhar (1977) assume that water use efficiency (λ), and therefore the g_1 parameter is constant over a given period of time, typically between a day and a growth season. This model assumes that a plant's stomata will always be operating at the lowest rate of g_s for a given rate of A and thus the function $\partial E/\partial A$ is minimized. Alternatively, hydraulic theory suggests that WUE may increase throughout the day as the "cost" of water increases due to increased evaporative demand, and the "demand" for carbon decreases due to water transport limitation (Katul et al. 2003). In this study we observed a lower mean g_0 and higher mean g_1 estimate from PM curves than for AM curves, suggesting that WUE decreased throughout the day, while stomatal behavior at low irradiance became more conservative. Here we explore two factors which may contribute to the observed diurnal trends in g_1 and g_0.

First, we observed an increase in $V_{cmax.25}$ from AM to PM (Table S2), which could influence our estimation of g_1 and g_0. In this study $V_{cmax.25}$ is fit using the "one-point method" (De Kauwe et al. 2016) either at ~08:00 (AM) or ~13:00 (PM), rather than traditional AC_i curves. In looking at the data used to estimate $V_{cmax.25}$ we see that when correcting for the effect of leaf temperature, rates of $A_{sat.25}$ are significantly different between AM and PM groups, with the AM group having lower mean $A_{sat.25}$ than the PM group. However, rates of C_i are not different between groups (Fig. S2), nor are uncorrected rates of A_{sat}, suggesting that the AM group may be facing a temperature limitation on activity of the enzyme Rubisco rather than a limitation due to the supply of carbon reaching the site of carboxylation (Harrison et al. 2010, Resco de Dios et al. 2016). This is further supported by the fact that mean rates of g_s are not different between AM and PM groups.

Many authors have reported an afternoon decline in $V_{cmax.25}$ (Singsaas et al. 2000, Kets et al. 2010, Nascimento and Marenco 2013, Stinziano et al. 2020), while an afternoon increase in $V_{cmax.25}$ is rather unusual. However, the afternoon increase may be the result of a more complete activation of Rubisco at the start of the PM measurement (~13:00) compared to the AM (~08:00) leading to a suppressed apparent maximum capacity in the AM group. Slow activation of Rubisco in *Populus* species has previously been observed (Roden and Pearcy 1993), as well as suppression of rates of activation after initial high light exposure (Kobza and Seemann 1989).

With a higher $V_{cmax.25}$ we would expect higher rates of A, which could lead to a lower g_1 and thus a higher iWUE if A and g_s did not increase in proportion. However, most plants maintain a fixed ratio of C_i to C_a as mesophyll requirements for photosynthesis create a tight coordination between A and g_s (Wong et al. 1985, Sharkey et al. 2007). Wong *et al.* (1979) also showed that this coordination is robust to changes in photosynthetic capacity, suggesting that changes in $V_{cmax.25}$ should not modulate the A:g_s relationship. We did not observe any significant differences in C_i

between AM and PM treatments at equivalent irradiance levels (Fig. S2), suggesting that while A may have increased due to higher $V_{cmax.25}$, g_s would have increased in proportion to facilitate the increased stomatal conductance to CO_2 (g_{sc}) (Farquhar et al. 1980), and thus the g_1 estimate should not have been effected.

A second possible explanation for the increase in g_1 between AM and PM and the decrease in g_0 from AM to PM is the effect of ambient conditions, both metrological and hydraulic, on the measured parameters. Previous field studies of diurnal rates of g_s and sap flux have demonstrated a strong link between canopy scale g_s and ambient VPD (Maruyama and Kuwagata 2008; Matthews et al. 2017; Miranda et al. 2013), with g_s declining in response to increased VPD. In addition, hydraulic supply theory suggest that at the leaf level for non-stressed plants, supply of water increases with increased evaporative demand (Buckley 2017; Damour et al. 2010), meaning that at the same rate of A more water is available, and g_s will be higher.

In our experiment we observed a rapid increase in ambient VPD from 06:00 to 12:30, and a decrease in ambient VPD from 12:31 to 18:00 (Fig. 5f). In addition, from previous studies on the same individuals we observed that early in the day xylem tension remains low, and levels off at mid-day levels from 12:30 onward (Serbin et al. 2020). This combination of increasing VPD and low xylem tension may serve to limit rates of g_s for AM leaves, causing them to appear more water use efficient in their stomatal behavior, as for the same rate of A, morning curves had lower g_s thus on average a higher fitted value for g_1 (Fig. 2c). Likewise for g_0, points from the AM curves were measured on or around solar noon, while for the PM curves, the g_0 points were measured around 18:30. When considering the ambient conditions at these two time points, it is not surprising that we see a 56% decrease in g_0 between AM and PM, as the ambient xylem flux at noon would be much higher than the flux late in the day when the solar zenith angle is much more obtuse (Fig.

6). This drop also follows the expectations of hydraulic supply and demand, which would assume a drop in g_0 over the diurnal course, concurrent with declining water reserves, and carbon demands (Duursma et al. 2019; Lombardozzi et al. 2017).

Finally, we do not believe that length of the measurement or differences in enclosure time are contributing to the patterns observed, as both AM and PM curves took approximately the same length of time to complete and were stepped through changes in irradiance at the same time.

Interaction of excision and time of day could reveal a progressive effect of hydraulic stress on stomatal parameters:

When the effect of treatment and time of day are jointly assessed, a temporal trend emerges. g_1 increases from AM to PM in both treatments, indicative of a time-of-day effect in both treatments. Interestingly, however, g_1 increases more for the intact branches than the cut branches between AM and PM (Fig. 2c). There are several possible explanations for this asymmetrical response. (1) It could be due to a bias in the amount of leaf area outside the measurement chamber, as intact branches had a significantly higher portion of their total leaf area experiencing ambient conditions than the cut treatment. (2) Due to hydraulic segmentation of woody tissue, the cumulative resistance across the water column of a cut branch will be lower than the resistance felt over the entire canopy of a tree (Pivovaroff et al. 2014), which would manifest in a greater diurnal hydraulic driving gradient for the intact treatment, and thus a comparably higher stomatal slope difference from AM to PM. (3) Cut branches have been disconnected from root soil moisture signaling, which may dampen natural diurnal dynamics in stomatal response related to ABA signaling or hydraulic conductivity (Christmann et al. 2007; Cochard et al. 1996; Huber et al. 2019). (4) The cutting of branches may have triggered the onset of xylem cavitation and failure

524 (Tyree and Sperry 1989). A reduction in xylem sapwood area would result in less water reaching
525 the leaves under the same xylem tension, as the total tension would be dispersed over a comparably
526 smaller xylem area. If less water was reaching the leaves, g_s would be lower and thus a lower g_1
527 estimate would be observed. It is possible that all four factors are working in concert to produce
528 the observed effect, however without xylem sapflow measurements, it is impossible to know
529 exactly what the driving dynamic is.

530 The other interesting temporal trend is the difference in excision effect from AM to PM. In the
531 AM group of plants, there was no significant difference in g_1 between cut and intact leaves, while
532 for the PM group, g_1 was 25% higher in the intact treatment than the cut treatment. This suggests
533 that while excision does not seem to bias the measurement results early in the day when the plants
534 are experiencing lower levels of water stress, as time goes on, the effect of excision becomes more
535 pronounced, leading the cut branches to exhibit a markedly more water use efficient stomatal
536 behavior. This response of increased iWUE, associated with stomatal limitation as a result of water
537 stress, has been well documented in the past (Franks et al. 1998, Klein 2014), and may either be
538 associated with embolism of the tissue adjacent to the cut (Tyree and Sperry 1989, Santiago and
539 Mulkey 2003), or a larger influence of hydraulic stress due to the removal of tissue and thus
540 material over which to resist xylem tension (Pivovaroff et al. 2014). This change in water use
541 efficiency is in line with our expectations that predawn cutting, along with significant storage or
542 wait time before a long response curve could alter the observed stomatal behavior, and thus bias
543 the parameter estimates obtained.

544 Interestingly however, g_0 does not follow the same pattern as g_1 with no statistical difference
545 in g_0 between excision treatments in the PM group, (albeit a 53% lower g_0 for the cut branches
546 than the intact branches). This suggests that the excision effect on stomata is more acutely seen at

higher g_s levels, and that both treatments are already behaving in a physiologically optimal fashion under low irradiance (Duursma et al. 2019). It has been well documented that maximum g_s is limited by leaf (Schulze and Hall 1982, Brodribb et al. 2003, Klein 2014) and soil (Thomas et al. 1999, Manzoni et al. 2011, Héroult et al. 2013) water stress, with the magnitude of the reduction in g_s larger at higher rates of conductance. Therefore if excision is contributing to hydraulic constraint within the xylem transport pathway, maximum g_s at high irradiance should be more acutely limited than g_s levels across all irradiance conditions (Anderegg et al. 2017).

There are several possible explanations for these treatment and temporal effects on g_0 and g_1. As mentioned before, the initial predawn cut may have been an impetus for xylem damage, which under increased diurnal xylem tension, continued to propagate throughout the day, becoming more acute in the PM treatment. "Runaway" cavitation and embolism of the xylem (Hölttä et al. 2009; Sperry et al. 1993; Tyree and Sperry 1989) effectively reduces the total xylem conduit area, limiting water supply to the leaves, and distributes the same amount of tension over less xylem area. These factors result in a reduction of apparent g_s rates compared to leaves supplied by intact xylem tissue, as less water is available at the site of conductance (Sperry et al. 1993).

Increased xylem tension also serves to decrease leaf water potential, which can trigger stomatal closure as Ψ_{leaf} approaches Ψ_{leaf} at turgor loss point (Martin-StPaul et al. 2017). This is especially apparent in species which behave more isohydric (Klein 2014), such as the poplar clone used in this study (Cocozza et al. 2010; Johnson et al. 2002). Isohydric plants are thought to have superior stomatal adjustment capacity compared with anisohydric plants, and as a consequence, more closely link their stomatal opening to ambient stress conditions, closing stomata at high VPD, and low Ψ_{leaf} or Ψ_{soil} (Klein 2014).

569 Alternatively, levels of abscisic acid (ABA) or another stress signaling hormone could have
570 been building over the day, with the effects becoming more pronounced for the PM group than the
571 AM group. Like Ψ_{leaf} influenced stomatal closure, hormonal stomatal closure is linked to an
572 external stressor such as leaf water stress, thermal stress, or excision stress (Tombesi et al. 2015;
573 Wilkinson and Davies 2002). The predicted isohydric response to any such stressor would be to
574 reduce stomatal aperture to safeguard against xylem damage and cellular turgor loss, both of which
575 are difficult to recover from, and costly in terms of carbon resource allocation (Klein et al. 2018;
576 McDowell et al. 2019).
577 When comparing between these two possible explanations for a lower g_s:A ratio for the PM
578 group, we find more evidence in support of hydraulic limitation than reduced stomatal aperture. In
579 previous studies of these individuals there were no detectable differences in Ψ_{leaf} or survey rates
580 of g_s from morning to midday (Serbin et al. 2020), suggesting that this species does not alter its
581 stomatal behavior in response to heat or moisture stress. A reduction in stomatal aperture while
582 maintaining the same rate of A would reduce C_i, as for the same rate of A less CO_2 is being supplied
583 to the site of carboxylation. However, we found no significant difference in either A or C_i between
584 any cut-intact pair at any level of irradiance (Fig. S2). This suggests that stomatal aperture and
585 thus g_{sc} was not affected by excision, leading hydraulic limitation to be the most plausible cause
586 of the effect observed, a similar finding to other excision studies (Santiago and Mulkey 2003,
587 Missik et al. 2021). This could also explain the incongruence between an effect on g_1 but not g_0,
588 as the effect of hydraulic limitation would be more acute under high irradiance, as xylem tension
589 scales with evaporative demand (Cai et al. 2020; Schulze et al. 1985; Tang and Boyer 2008).
590
591 <u>Impact of parameter assumptions on leaf-level simulations:</u>

Results from simulations of hybrid poplar using our coupled assimilation, stomatal conductance, and energy balance model revealed that methodological choice in parametrization resulted in significant differences in both the diurnal pattern of g_s, and the integrated transpiration over a simulated diurnal cycle (Fig. 5, Fig. S1). Simulated rates of A and g_s correspond closely to previous studies of poplar species which find mean rates of A at 20 µmol m^{-2} s^{-1} and g_s at 0.35 mol m^{-2} s^{-1} (Bernacchi, et al. 2003a, Cseke et al. 2009, Rogers et al. 2012). Across all six simulations, g_s rates exhibited a marked midday decline, which is brought on by an increased VPD as the air warms (El-Sharkaway and Cock 1984, Dai et al. 1992, Tardieu and Davies 1993, Merilo et al. 2018). This decline in g_s results in stomatal limitation on A, regulating the shape of the photosynthetic response (Bernacchi, et al. 2003a). The use of a dynamic simulation reveals that the parameters g_0 and g_1 strongly regulate both E and A, as an afternoon increase in g_1 leads to a nearly 33% increase in rates of g_s. As expected, the parametrizations which resulted in higher fitted values of g_1 and g_0, produced higher sustained simulated rates of both g_s and A, while still maintaining the same pronounced overall diurnal pattern representative of irradiance and VPD trends (Fig. 5a). When considering total transpiration over a diurnal (06:00-18:30) period, choice of parametrization has a strong effect on the total level of transpiration in poplar, with values ranging from 2.73 L m^{-2} day^{-1} for the AM-cut treatment, to 3.32 L m^{-2} day^{-1} for the PM-intact treatment (Fig. 5c). While this difference is small compared to the day-to-day variation expected in E (Bauerle et al. 2009), this consistent 18% difference taken over a full growth season would represent a large uncertainty in the rate of transpiration of a plant canopy. In addition, the two predictions from the intact treatment (and their associated error) are largely different, suggesting that choice regarding time of day of measurement has serious ramifications on g_1 and g_0 in poplar, as well as predicted model output.

615

616 Conclusions:

617 In ecophysiology it is often necessary to assume that single leaf, ex situ measurements of gas
618 exchange are broadly comparable to in situ, whole canopy dynamics, if the proper precautions
619 (e.g., predawn excision and recutting under water) are taken, and assumptions (e.g., the hydraulic
620 dynamics of a cut branch are equivalent to an intact branch) are minimized. While it has been
621 shown that ex situ measurement does not alter photosynthesis (Verryckt et al. 2020) and may even
622 be the better option for AC_i curves (Ainsworth et al. 2003), it is currently unknown what approach
623 is most suitable for long duration response curves used to estimate g_1 (Damour et al. 2010) and g_0
624 (Duursma et al. 2019). Here we show that in cases where measurements are made early in the day,
625 or a short time post excision, ex situ stomatal response parameters estimated from ex situ response
626 curves match those obtained from in situ response curves (Fig. 3). However, we also demonstrate
627 that choices regarding experimental design, and failure to consider the strong diurnal effect on
628 hydraulic driving gradients can confound comparisons of results (Fig. 5).

629 While this study only investigated stomatal dynamics in a single isohydric woody species, we
630 none the less show that if the aim of stomatal response curves is to ascertain a single nominal value
631 for a species or group of interest, the exact sampling method must be carefully considered. It may
632 be preferable to average measurements across the diurnal period, rather than conduct all curves at
633 one time point during the day. If the time since excision is not recorded, conclusions about plant
634 to plant or species to species differences in parameters may be of limited value. Therefore, failure
635 to consider potential stomatal parameter measurement uncertainties, together with other
636 uncertainties and known variation in parameters across space and time, on downstream leaf-,

canopy-, and ecosystem-scale processes, have the potential to introduce considerable uncertainties into the modeling of plant carbon and water cycling (Dietze et al. 2014; Rogers et al. 2017)

Data and Materials Availability:

All data will be made publicly available upon acceptance of the manuscript and a DOI will be provided.

Supplementary Data:

One supporting document (Supplemental_Data.docx) containing Table S1, S2, and S3 and Figures S1, and S2 as referenced in the text.

Conflict of Interest:

None declared.

Funding:

This work was supported by the Next-Generation Ecosystem Experiments–Tropics project supported by the U.S. DOE, Office of Science, Office of Biological and Environmental Research, and through the United States Department of Energy contract No. DE- SC0012704 to Brookhaven National Laboratory.

Acknowledgements:

We would like to thank Justin Andrews and Jeremiah Anderson for their assistance with plant care. We are grateful to Keith Lewin for his invaluable expertise during the planting of experimental saplings.

Author's Contributions:

KJD and JL conceived of and designed the study. All authors contributed to methodology development. KJD executed the experiment, collected data, conducted data analysis, and wrote the manuscript with contributions from JL, AR, and SPS.

References:

Ainsworth EA, Davey PA, Hymus GJ, Osborne CP, Rogers A, Blum H, Nösberger J, Long SP (2003) Is stimulation of leaf photosynthesis by elevated carbon dioxide concentration maintained in the long term? A test with *Lolium perenne* grown for 10 years at two nitrogen fertilization levels under *F* ree *A* ir *C* O $_2$ *E* nrichment (FACE): Photosynthetic acclimation of *L. perenne* to elevated [CO $_2$]. Plant Cell Environ 26:705–714. https://doi.org/10.1046/j.1365-3040.2003.01007.x

Akalusi ME, Meng F, P.-A. Bourque C (2021) Photosynthetic parameters and stomatal conductance in attached and detached balsam fir foliage. Plant-Environ Interact 2:206–215. https://doi.org/10.1002/pei3.10059

Anderegg WRL, Wolf A, Arango-Velez A, Choat B, Chmura DJ, Jansen S, Kolb T, Li S, Meinzer F, Pita P, Resco de Dios V, Sperry JS, Wolfe BT, Pacala S (2017) Plant water potential improves prediction of empirical stomatal models Aroca R (ed). PLOS ONE 12:e0185481. https://doi.org/10.1371/journal.pone.0185481

Ball TJ, Woodrow IE, Berry JA (1987) A Model Predicting Stomatal Conductance and its Contribution to the Control of Photosynthesis under Different Environmental Conditions. In: Biggins J (ed) Progress in photosynthesis research. Springer, Dordrecht, pp 221–224.

Bauerle WL, Bowden JD, Wang GG, Shahba MA (2009) Exploring the importance of within-canopy spatial temperature variation on transpiration predictions. J Exp Bot 60:3665–3676. https://doi.org/10.1093/jxb/erp206

687 Bernacchi CJ, Bagley JE, Serbin SP, Ruiz-Vera UM, Rosenthal DM, Vanloocke A (2013)
688 Modelling C 3 photosynthesis from the chloroplast to the ecosystem: Scaling photosynthesis
689 using models. Plant Cell Environ 36:1641–1657. https://doi.org/10.1111/pce.12118

690 Bernacchi CJ, Calfapietra C, Davey PA, Wittig VE, Scarascia-Mugnozza GE, Raines CA, Long
691 SP (2003) Photosynthesis and Stomatal Conductance Responses of Poplars to Free-Air CO_2
692 Enrichment (PopFACE) during the First Growth Cycle and Immediately Following Coppice.
693 New Phytol 159:609–621.

694 Bernacchi CJ, Pimentel C, Long SP (2003) *In vivo* temperature response functions of parameters
695 required to model RuBP-limited photosynthesis: Modelling RuBP-limited photosynthesis.
696 Plant Cell Environ 26:1419–1430. https://doi.org/10.1046/j.0016-8025.2003.01050.x

697 Bernacchi CJ, Singsaas EL, Pimentel C, Portis Jr AR, Long SP (2001) Improved temperature
698 response functions for models of Rubisco-limited photosynthesis: *In vivo* Rubisco enzyme
699 kinetics. Plant Cell Environ 24:253–259. https://doi.org/10.1111/j.1365-3040.2001.00668.x

700 Blackman CJ, Pfautsch S, Choat B, Delzon S, Gleason SM, Duursma RA (2016) Toward an
701 index of desiccation time to tree mortality under drought: Desiccation time to tree mortality.
702 Plant Cell Environ 39:2342–2345. https://doi.org/10.1111/pce.12758

703 Brodribb TJ, Holbrook NM, Edwards EJ, Gutiérrez MV (2003) Relations between stomatal
704 closure, leaf turgor and xylem vulnerability in eight tropical dry forest trees: Stomatal closure
705 and xylem cavitation. Plant Cell Environ 26:443–450. https://doi.org/10.1046/j.1365-
706 3040.2003.00975.x

707 Buckley TN (2017) Modeling Stomatal Conductance. Plant Physiol 174:572–582.
708 https://doi.org/10.1104/pp.16.01772

709 Burnett AC, Davidson KJ, Serbin SP, Rogers A (2019) The "one-point method" for estimating
710 maximum carboxylation capacity of photosynthesis: A cautionary tale. Plant Cell Environ
711 42:2472–2481. https://doi.org/10.1111/pce.13574

712 Burnett AC, Serbin SP, Lamour J, Anderson J, Davidson KJ, Yang D, Rogers A (2021) Seasonal
713 trends in photosynthesis and leaf traits in scarlet oak. Tree Physiol.
714 https://doi.org/10.1093/treephys/tpab015

715 Cai G, Ahmed MA, Dippold MA, Zarebanadkouki M, Carminati A (2020) Linear relation
716 between leaf xylem water potential and transpiration in pearl millet during soil drying. Plant
717 Soil 447:565–578. https://doi.org/10.1007/s11104-019-04408-z

718 Christmann A, Weiler EW, Steudle E, Grill E (2007) A hydraulic signal in root-to-shoot
719 signalling of water shortage: Hydraulic signalling of water shortage. Plant J 52:167–174.
720 https://doi.org/10.1111/j.1365-313X.2007.03234.x

721 Cochard H, Bréda N, Granier A (1996) Whole tree hydraulic conductance and water loss
722 regulation in Quercus during drought: evidence for stomatal control of embolism? Ann Sci
723 For 53:197–206. https://doi.org/10.1051/forest:19960203

724 Cocozza C, Cherubini P, Regier N, Saurer M, Frey B, Tognetti R (2010) Early effects of water
725 deficit on two parental clones of Populus nigra grown under different environmental
726 conditions. Funct Plant Biol 37:244. https://doi.org/10.1071/FP09156

727 Cowan IR (1978) Stomatal Behaviour and Environment. In: Preston RD, Woolhouse HW (eds)
728 Advances in Botanical Research. Academic Press, pp 117–228.
729 https://doi.org/10.1016/S0065-2296(08)60370-5

730 Cowan IR, Fraquhar GD (1977) Stomatal function in relation to leaf metabolism and
731 environment. In: Symposia of the Society for Experimental Biology.pp 471–505.

732 Cseke LJ, Tsai C, Rogers A, Nelsen MP, White HL, Karnosky DF, Podila GK (2009)
733 Transcriptomic comparison in the leaves of two aspen genotypes having similar carbon
734 assimilation rates but different partitioning patterns under elevated [CO_2]. New Phytol
735 182:891–911. https://doi.org/10.1111/j.1469-8137.2009.02812.x

736 Dai Z, Edwards GE, Ku MSB (1992) Control of Photosynthesis and Stomatal Conductance in
737 *Ricinus communis* L. (Castor Bean) by Leaf to Air Vapor Pressure Deficit. Plant Physiol
738 99:1426–1434. https://doi.org/10.1104/pp.99.4.1426

739 Damour G, Simonneau T, Cochard H, Urban L (2010) An overview of models of stomatal
740 conductance at the leaf level: Models of stomatal conductance. Plant Cell Environ 39:1419–
741 1438. https://doi.org/10.1111/j.1365-3040.2010.02181.x

742 De Kauwe MG, Lin Y-S, Wright IJ, Medlyn BE, Crous KY, Ellsworth DS, Maire V, Prentice IC,
743 Atkin OK, Rogers A, Niinemets Ü, Serbin SP, Meir P, Uddling J, Togashi HF, Tarvainen L,
744 Weerasinghe LK, Evans BJ, Ishida FY, Domingues TF (2016) A test of the 'one-point
745 method' for estimating maximum carboxylation capacity from field-measured, light-
746 saturated photosynthesis. New Phytol 210:1130–1144. https://doi.org/10.1111/nph.13815

747 Dietze MC, Serbin SP, Davidson C, Desai AR, Feng X, Kelly R, Kooper R, LeBauer D,
748 Mantooth J, McHenry K, Wang D (2014) A quantitative assessment of a terrestrial biosphere
749 model's data needs across North American biomes: PEcAn/ED model-data uncertainty
750 analysis. J Geophys Res Biogeosciences 119:286–300.
751 https://doi.org/10.1002/2013JG002392

752 Drake PL, Froend RH, Franks PJ (2013) Smaller, faster stomata: scaling of stomatal size, rate of
753 response, and stomatal conductance. J Exp Bot 64:495–505.
754 https://doi.org/10.1093/jxb/ers347

755 Duursma RA, Blackman CJ, Lopéz R, Martin-StPaul NK, Cochard H, Medlyn BE (2019) On the
756 minimum leaf conductance: its role in models of plant water use, and ecological and
757 environmental controls. New Phytol 221:693–705. https://doi.org/10.1111/nph.15395

758 El-Sharkaway MA, Cock JH (1984) Water Use Efficiency of Cassava. I. Effects of Air Humidity
759 and Water Stress on Stomatal Conductance and Gas Exchange1. Crop Sci
760 24:cropsci1984.0011183X002400030017x.
761 https://doi.org/10.2135/cropsci1984.0011183X002400030017x

762 Erickson RO, Michelini FL (1957) THE PLASTOCHRON INDEX. Am J Bot 44:297–305.
763 https://doi.org/10.2307/2438380

764 Farquhar GD, von Caemmerer S, Berry JA (1980) A biochemical model of photosynthetic CO2
765 assimilation in leaves of C3 species. Planta 149:78–90. https://doi.org/10.1007/BF00386231

766 Franks PJ, Cowan 1 2 I. R., Farquhar GD (1998) A study of stomatal mechanics using the cell
767 pressure probe. Plant Cell Environ 21:94–100. https://doi.org/10.1046/j.1365-
768 3040.1998.00248.x

769 Harrison MT, Kelman WM, Moore AD, Evans JR (2010) Grazing winter wheat relieves plant
770 water stress and transiently enhances photosynthesis. Funct Plant Biol 37:726–736.

771 Héroult A, Lin Y-S, Bourne A, Medlyn BE, Ellsworth DS (2013) Optimal stomatal conductance
772 in relation to photosynthesis in climatically contrasting *Eucalyptus* species under drought:
773 Stomatal responses of eucalyptus under drought. Plant Cell Environ 36:262–274.
774 https://doi.org/10.1111/j.1365-3040.2012.02570.x

775 Hetherington AM, Woodward FI (2003) The role of stomata in sensing and driving
776 environmental change. Nature 424:901–908. https://doi.org/10.1038/nature01843

777 Hölttä T, Cochard H, Nikinmaa E, Mencuccini M (2009) Capacitive effect of cavitation in xylem
778 conduits: results from a dynamic model. Plant Cell Environ 32:10–21.
779 https://doi.org/10.1111/j.1365-3040.2008.01894.x

780 Huber AE, Melcher PJ, Piñeros MA, Setter TL, Bauerle TL (2019) Signal coordination before,
781 during and after stomatal closure in response to drought stress. New Phytol 224:675–688.
782 https://doi.org/10.1111/nph.16082

783 Johnson JD, Tognetti R, Paris P (2002) Water relations and gas exchange in poplar and willow
784 under water stress and elevated atmospheric CO 2. Physiol Plant 115:93–100.
785 https://doi.org/10.1034/j.1399-3054.2002.1150111.x

786 Katul G, Leuning R, Oren R (2003) Relationship between plant hydraulic and biochemical
787 properties derived from a steady-state coupled water and carbon transport model: Plant
788 hydraulic and biochemical properties. Plant Cell Environ 26:339–350.
789 https://doi.org/10.1046/j.1365-3040.2003.00965.x

790 Katul G, Manzoni S, Palmroth S, Oren R (2010) A stomatal optimization theory to describe the
791 effects of atmospheric CO2 on leaf photosynthesis and transpiration. Ann Bot 105:431–442.
792 https://doi.org/10.1093/aob/mcp292

793 Kerstiens G (1996) Cuticular water permeability and its physiological significance. J Exp Bot
794 47:1813–1832. https://doi.org/10.1093/jxb/47.12.1813

795 Kets K, Darbah JNT, Sober A, Riikonen J, Sober J, Karnosky DF (2010) Diurnal changes in
796 photosynthetic parameters of Populus tremuloides, modulated by elevated concentrations of

797 CO2 and/or O3 and daily climatic variation. Environ Pollut 158:1000–1007.
798 https://doi.org/10.1016/j.envpol.2009.09.001

799 Klein T (2014) The variability of stomatal sensitivity to leaf water potential across tree species
800 indicates a continuum between isohydric and anisohydric behaviours Niu S (ed). Funct Ecol
801 28:1313–1320. https://doi.org/10.1111/1365-2435.12289

802 Klein T, Zeppel MJB, Anderegg WRL, Bloemen J, De Kauwe MG, Hudson P, Ruehr NK,
803 Powell TL, von Arx G, Nardini A (2018) Xylem embolism refilling and resilience against
804 drought-induced mortality in woody plants: processes and trade-offs. Ecol Res.
805 https://doi.org/10.1007/s11284-018-1588-y

806 Kobza J, Seemann JR (1989) Regulation of Ribulose-1,5-Bisphosphate Carboxylase Activity in
807 Response to Diurnal Changes in Irradiance. Plant Physiol 89:918.
808 https://doi.org/10.1104/pp.89.3.918

809 Lamour J, Serbin SP (2021) LeafGasExchange.

810 Lawson T, Blatt MR (2014) Stomatal Size, Speed, and Responsiveness Impact on Photosynthesis
811 and Water Use Efficiency. Plant Physiol 164:1556–1570.
812 https://doi.org/10.1104/pp.114.237107

813 Lawson T, Kramer DM, Raines CA (2012) Improving yield by exploiting mechanisms
814 underlying natural variation of photosynthesis. Curr Opin Biotechnol 23:215–220.
815 https://doi.org/10.1016/j.copbio.2011.12.012

816 Lawson T, Vialet-Chabrand S (2019) Speedy stomata, photosynthesis and plant water use
817 efficiency. New Phytol 221:93–98. https://doi.org/10.1111/nph.15330

818 Leakey ADB, Bernacchi CJ, Ort DR, Long SP (2006) Long-term growth of soybean at elevated
819 [CO2] does not cause acclimation of stomatal conductance under fully open-air conditions.
820 Plant Cell Environ 29:1794–1800. https://doi.org/10.1111/j.1365-3040.2006.01556.x

821 Lenth R, Singmann H, Love J, Buerkner P, Herve M (2020) Estimated Marginal Means, aka
822 Least-Squares Means.

823 Leuning R (1995) A critical appraisal of a combined stomatal-photosynthesis model for C3
824 plants. Plant Cell Environ 18:339–355. https://doi.org/10.1111/j.1365-3040.1995.tb00370.x

825 Leuning R (2002) Temperature dependence of two parameters in a photosynthesis model:
826 Temperature dependence of photosynthetic parameters. Plant Cell Environ 25:1205–1210.
827 https://doi.org/10.1046/j.1365-3040.2002.00898.x

828 Lin Y-S, Medlyn BE, Duursma RA, Prentice IC, Wang H, Baig S, Eamus D, de Dios VR,
829 Mitchell P, Ellsworth DS, de Beeck MO, Wallin G, Uddling J, Tarvainen L, Linderson M-L,
830 Cernusak LA, Nippert JB, Ocheltree TW, Tissue DT, Martin-StPaul NK, Rogers A, Warren
831 JM, De Angelis P, Hikosaka K, Han Q, Onoda Y, Gimeno TE, Barton CVM, Bennie J, Bonal
832 D, Bosc A, Löw M, Macinins-Ng C, Rey A, Rowland L, Setterfield SA, Tausz-Posch S,

Zaragoza-Castells J, Broadmeadow MSJ, Drake JE, Freeman M, Ghannoum O, Hutley LB, Kelly JW, Kikuzawa K, Kolari P, Koyama K, Limousin J-M, Meir P, Lola da Costa AC, Mikkelsen TN, Salinas N, Sun W, Wingate L (2015) Optimal stomatal behaviour around the world. Nat Clim Change 5:459–464. https://doi.org/10.1038/nclimate2550

Lombardozzi DL, Zeppel MJB, Fisher RA, Tawfik A (2017) Representing nighttime and minimum conductance in CLM4.5: global hydrology and carbon sensitivity analysis using observational constraints. Geosci Model Dev 10:321–331. https://doi.org/10.5194/gmd-10-321-2017

Machado R, Loram-Lourenço L, Farnese FS, Alves RDFB, Sousa LF, Silva FG, Filho SCV, Torres-Ruiz JM, Cochard H, Menezes-Silva PE (2021) Where do leaf water leaks come from? Trade-offs underlying the variability in minimum conductance across tropical savanna species with contrasting growth strategies. New Phytol 229:1415–1430. https://doi.org/10.1111/nph.16941

Manzoni S, Vico G, Katul G, Fay PA, Polley W, Palmroth S, Porporato A (2011) Optimizing stomatal conductance for maximum carbon gain under water stress: a meta-analysis across plant functional types and climates: Optimal leaf gas exchange under water stress. Funct Ecol 25:456–467. https://doi.org/10.1111/j.1365-2435.2010.01822.x

Martin-StPaul N, Delzon S, Cochard H (2017) Plant resistance to drought depends on timely stomatal closure Maherali H (ed). Ecol Lett 20:1437–1447. https://doi.org/10.1111/ele.12851

Maruyama A, Kuwagata T (2008) Diurnal and seasonal variation in bulk stomatal conductance of the rice canopy and its dependence on developmental stage. Agric For Meteorol 148:1161–1173. https://doi.org/10.1016/j.agrformet.2008.03.001

Matthews JSA, Vialet-Chabrand SRM, Lawson T (2017) Diurnal Variation in Gas Exchange: The Balance between Carbon Fixation and Water Loss. Plant Physiol 174:614–623. https://doi.org/10.1104/pp.17.00152

McAusland L, Vialet-Chabrand S, Davey P, Baker NR, Brendel O, Lawson T (2016) Effects of kinetics of light-induced stomatal responses on photosynthesis and water-use efficiency. New Phytol 211:1209–1220. https://doi.org/10.1111/nph.14000

McDowell NG, Brodribb TJ, Nardini A (2019) Hydraulics in the 21 st century. New Phytol 224:537–542. https://doi.org/10.1111/nph.16151

Medlyn BE, Duursma RA, Eamus D, Ellsworth DS, Prentice IC, Barton CVM, Crous KY, De Angelis P, Freeman M, Wingate L (2011) Reconciling the optimal and empirical approaches to modelling stomatal conductance. Glob Change Biol 17:2134–2144. https://doi.org/10.1111/j.1365-2486.2010.02375.x

Meicenheimer RD (2014) The plastochron index: Still useful after nearly six decades. Am J Bot 101:1821–1835. https://doi.org/10.3732/ajb.1400305

Merilo E, Yarmolinsky D, Jalakas P, Parik H, Tulva I, Rasulov B, Kilk K, Kollist H (2018) Stomatal VPD Response: There Is More to the Story Than ABA. Plant Physiol 176:851–864. https://doi.org/10.1104/pp.17.00912

Miner GL, Bauerle WL, Baldocchi DD (2017) Estimating the sensitivity of stomatal conductance to photosynthesis: a review: The sensitivity of conductance to photosynthesis. Plant Cell Environ 40:1214–1238. https://doi.org/10.1111/pce.12871

Miranda T, Ebner M, Traiser C, Roth-Nebelsick A (2013) Diurnal pattern of stomatal conductance in the large-leaved temperate liana Aristolochia macrophylla depends on spatial position within the leaf lamina. Ann Bot 111:905–915. https://doi.org/10.1093/aob/mct061

Missik JEC, Oishi AC, Benson MC, Meretsky VJ, Phillips RP, Novick KA (2021) Performing gas-exchange measurements on excised branches - evaluation and recommendations. Photosynthetica 59:61–73. https://doi.org/10.32615/ps.2020.079

Mott KA (1988) Do Stomata Respond to CO_2 Concentrations Other than Intercellular? Plant Physiol 86:200–203. https://doi.org/10.1104/pp.86.1.200

Muir CD (2019) Tealeaves: An R package for modelling leaf temperature using energy budgets. AoB PLANTS 11:1–10. https://doi.org/10.1093/aobpla/plz054

Muir CD (2020) tealeaves: an R package for modelling leaf temperature using energy budgets.

Nascimento HCS, Marenco RA (2013) Mesophyll conductance variations in response to diurnal environmental factors in Myrcia paivae and Minquartia guianensis in Central Amazonia. Photosynthetica 51:457–464. https://doi.org/10.1007/s11099-013-0046-x

Pinheiro J, Bates D, DebRoy S, Sarkar D, Heisterkamp S, Bert VW (2020) Package 'nlme'.

Pivovaroff AL, Sack L, Santiago LS (2014) Coordination of stem and leaf hydraulic conductance in southern California shrubs: a test of the hydraulic segmentation hypothesis. New Phytol 203:842–850. https://doi.org/10.1111/nph.12850

R Core Team (2013) R: A language and environment for statistical computing. R Foundation for Statistical Computing, Vienna, Austria.

Resco de Dios V, Anderegg WRL, Li X, Tissue DT, Bahn M, Landais D, Milcu A, Yao Y, Nolan RH, Roy J, Gessler A (2020) Circadian Regulation Does Not Optimize Stomatal Behaviour. Plants 9:1091. https://doi.org/10.3390/plants9091091

Resco de Dios V, Loik ME, Smith R, Aspinwall MJ, Tissue DT (2016) Genetic variation in circadian regulation of nocturnal stomatal conductance enhances carbon assimilation and growth: On the function of nocturnal stomatal conductance. Plant Cell Environ 39:3–11. https://doi.org/10.1111/pce.12598

902 Ricciuto D, Sargsyan K, Thornton P (2018) The Impact of Parametric Uncertainties on
903 Biogeochemistry in the E3SM Land Model. J Adv Model Earth Syst 10:297–319.
904 https://doi.org/10.1002/2017MS000962

905 Roden JS, Pearcy RW (1993) Photosynthetic gas exchange response of poplars to steady-state
906 and dynamic light environments. Oecologia 93:208–214.
907 https://doi.org/10.1007/BF00317673

908 Rogers A, McDonald K, Muehlbauer MF, Hoffman A, Koenig K, Newman L, Taghavi S, Lelie
909 D (2012) Inoculation of hybrid poplar with the endophytic bacterium Enterobacter sp. 638
910 increases biomass but does not impact leaf level physiology. GCB Bioenergy 4:364–370.
911 https://doi.org/10.1111/j.1757-1707.2011.01119.x

912 Rogers A, Medlyn BE, Dukes JS, Bonan G, von Caemmerer S, Dietze MC, Kattge J, Leakey
913 ADB, Mercado LM, Niinemets Ü, Prentice IC, Serbin SP, Sitch S, Way DA, Zaehle S (2017)
914 A roadmap for improving the representation of photosynthesis in Earth system models. New
915 Phytol 213:22–42. https://doi.org/10.1111/nph.14283

916 Salvucci ME, Anderson JC (1987) Factors Affecting the Activation State and the Level of Total
917 Activity of Ribulose Bisphosphate Carboxylase in Tobacco Protoplasts. Plant Physiol 85:66–
918 71. https://doi.org/10.1104/pp.85.1.66

919 Santiago LS, Mulkey SS (2003) A Test of Gas Exchange Measurements on Excised Canopy
920 Branches of Ten Tropical Tree Species. Photosynthetica 41:343–347.
921 https://doi.org/10.1023/B:PHOT.0000015457.92479.eb

922 Schulze E-D, Čermák J, Matyssek M, Penka M, Zimmermann R, Vasicek F, Gries W, Kučera J
923 (1985) Canopy transpiration and water fluxes in the xylem of the trunk of Larix and Picea
924 trees—a comparison of xylem flow, porometer and cuvette measurements. Oecologia
925 66:475–483.

926 Schulze E-D, Hall AE (1982) Stomatal Responses, Water Loss and CO2 Assimilation Rates of
927 Plants in Contrasting Environments. In: Lange OL, Nobel PS, Osmond CB, Ziegler H (eds)
928 Physiological Plant Ecology II: Water Relations and Carbon Assimilation. Springer Berlin
929 Heidelberg, Berlin, Heidelberg, pp 181–230. https://doi.org/10.1007/978-3-642-68150-9_8

930 Serbin SP, Anderson JA, Davidson KJ, Rogers A (2020) Combining plant physiology and
931 remote sensing to enable detection of concealed activities that are sensed through overlying
932 vegetation. Defense Advanced Research Projects Agency. Biological Technologies Office.

933 Serbin SP, Singh A, McNeil BE, Kingdon CC, Townsend PA (2014) Spectroscopic
934 determination of leaf morphological and biochemical traits for northern temperate and boreal
935 tree species. Ecol Appl 24:1651–1669. https://doi.org/10.1890/13-2110.1

936 Sharkey TD, Bernacchi CJ, Farquhar GD, Singsaas EL (2007) Fitting photosynthetic carbon
937 dioxide response curves for C 3 leaves. Plant Cell Environ 30:1035–1040.
938 https://doi.org/10.1111/j.1365-3040.2007.01710.x

939 Singsaas EL, Ort DR, DeLUCIA EH (2000) Diurnal regulation of photosynthesis in understory
940 saplings: Diurnal regulation of photosynthesis. New Phytol 145:39–49.
941 https://doi.org/10.1046/j.1469-8137.2000.00556.x

942 Sperry JS (2013) Cutting-edge research or cutting-edge artefact? An overdue control experiment
943 complicates the xylem refilling story: Xylem-refilling artefacts. Plant Cell Environ 36:1916–
944 1918. https://doi.org/10.1111/pce.12148

945 Sperry JS, Alder NN, Eastlack SE (1993) The Effect of Reduced Hydraulic Conductance on
946 Stomatal Conductance and Xylem Cavitation. J Exp Bot 44:1075–1082.
947 https://doi.org/10.1093/jxb/44.6.1075

948 Stinziano J, Harjoe M, Roback C, Toliver N, Rogers A, Hanson DT (2020) Photosynthetic
949 capacity exhibits diurnal variation, implications for terrestrial biosphere models and gas
950 exchange measurements. Preprints. https://doi.org/10.22541/au.160133681.10036922

951 Tang A-C, Boyer JS (2008) Xylem tension affects growth-induced water potential and daily
952 elongation of maize leaves. J Exp Bot 59:753–764. https://doi.org/10.1093/jxb/erm371

953 Tardieu F, Davies WJ (1993) Integration of hydraulic and chemical signalling in the control of
954 stomatal conductance and water status of droughted plants. Plant Cell Environ 16:341–349.
955 https://doi.org/10.1111/j.1365-3040.1993.tb00880.x

956 Thomas DS, Eamus D, Bell D (1999) Optimization theory of stomatal behaviour: II. Stomatal
957 responses of several tree species of north Australia to changes in light, soil and atmospheric
958 water content and temperature. J Exp Bot 50:393–400.
959 https://doi.org/10.1093/jxb/50.332.393

960 Tombesi S, Nardini A, Frioni T, Soccolini M, Zadra C, Farinelli D, Poni S, Palliotti A (2015)
961 Stomatal closure is induced by hydraulic signals and maintained by ABA in drought-stressed
962 grapevine. Sci Rep 5:12449. https://doi.org/10.1038/srep12449

963 Tukey JW (1949) Comparing Individual Means in the Analysis of Variance. Biometrics 5:99.
964 https://doi.org/10.2307/3001913

965 Tyree MT, Sperry JS (1989) Vulnerability of Xylem to Cavitation and Embolism. Annu Rev
966 Plant Biol 40:19–36.

967 Venturas MD, Mackinnon ED, Jacobsen AL, Pratt RB (2015) Excising stem samples underwater
968 at native tension does not induce xylem cavitation: No evidence for a tension-cutting artefact.
969 Plant Cell Environ 38:1060–1068. https://doi.org/10.1111/pce.12461

970 Verryckt LT, Van Langenhove L, Ciais P, Courtois EA, Vicca S, Peñuelas J, Stahl C, Coste S,
971 Ellsworth DS, Posada JM, Obersteiner M, Chave J, Janssens IA (2020) Coping with branch
972 excision when measuring leaf net photosynthetic rates in a lowland tropical forest. Biotropica
973 52:608–615. https://doi.org/10.1111/btp.12774

Von Caemmerer S (2013) Steady-state models of photosynthesis: Steady-state models of photosynthesis. Plant Cell Environ 36:1617–1630. https://doi.org/10.1111/pce.12098

Walker AP, Johnson AL, Rogers A, Anderson J, Bridges RA, Fisher RA, Lu D, Ricciuto DM, Serbin SP, Ye M (2021) Multi-hypothesis comparison of Farquhar and Collatz photosynthesis models reveals the unexpected influence of empirical assumptions at leaf and global scales. Glob Change Biol 27:804–822. https://doi.org/10.1111/gcb.15366

Wheeler JK, Huggett BA, Tofte AN, Rockwell FE, Holbrook NM (2013) Cutting xylem under tension or supersaturated with gas can generate PLC and the appearance of rapid recovery from embolism: Sampling induced embolism. Plant Cell Environ 36:1938–1949. https://doi.org/10.1111/pce.12139

Wilkinson S, Davies WJ (2002) ABA-based chemical signalling: the co-ordination of responses to stress in plants: ABA-based chemical signalling. Plant Cell Environ 25:195–210. https://doi.org/10.1046/j.0016-8025.2001.00824.x

Williamson VG, Milburn JA (1995) Cavitation events in cut stems kept in water: implications for cut flower senescence. Sci Hortic 64:219–232. https://doi.org/10.1016/0304-4238(95)00842-X

Wolfe BT, Sperry JS, Kursar TA (2016) Does leaf shedding protect stems from cavitation during seasonal droughts? A test of the hydraulic fuse hypothesis. New Phytol 212:1007–1018.

Wong SC, Cowan IR, Farquhar GD (1979) Stomatal conductance correlates with photosynthetic capacity. Nature 282:424–426. https://doi.org/10.1038/282424a0

Wong SC, Cowan IR, Farquhar GD (1985) Leaf Conductance in Relation to Rate of CO2 Assimilation. Plant Physiol 78:821–825. https://doi.org/10.1104/pp.78.4.821

Wu J, Serbin SP, Ely KS, Wolfe BT, Dickman LT, Grossiord C, Michaletz ST, Collins AD, Detto M, McDowell NG, Wright SJ, Rogers A (2019) The response of stomatal conductance to seasonal drought in tropical forests. Glob Change Biol 26:823–839. https://doi.org/10.1111/gcb.14820

Figure Legends:

Figure 1. Overall format of the stomatal response curve approach in which irradiance is reduced in a stepwise manner, and rates of g_s decline in response. (a) Example of a curve in which rates of g_s reached steady state at each light level. Red points on the response curve correspond to the mean value for that irradiance level extracted for subsequent analysis. Even at steady state levels of g_s,

there is still a great degree of observation-to-observation variation. (b) Standard visualization of the data from the curve conducted in (a). Plotting this way allows for a linear approximation of the g_1 and g_0 parameters, which are the slope and intercept respectively of the best fit line.

Figure 2. Effect of (a) excision and (b) time of day, and their interaction (c) on the fitted value of g_1 from the USO model, when g_0 is set to $g_{0,population}$ (0.037 mol m^2s^{-1}). Both excision and time of day produced a significant fixed effects relationship, with a 10% reduction in estimated g_1 for excised branches (a), and an 89% increase in g_1 from the AM treatment to the PM treatment (b). For the interaction (c) all contrast level differences are significant, except for the difference between cut and intact treatments during the AM time period. Notably, for the PM time period, predicted g_1 for the cut treatment was 25% less than the intact treatment, suggesting that the measurements are not comparable. Points connected by a colored line indicate that they were collected together as part of the same response curve. Points of the same color have the same random effects structure applied. Grey vertical line denotes the point of light compensation (A_n = 0).

Figure 3. Comparisons of the interactive effects of excision and time of day on stomatal parameters. Percent difference between all six linear contrasts and absolute values and their error for (a-b) g_0 estimates, (c-d) g_1 estimates, and (e-f) g_1 estimates when g_0 is set to $g_{0,population}$. All differences reported in panels a, c, and e by percentage are significant. Error bars in panels b, d, and f are ± 2 SE, n=8. Full statistics and values for all effects are reported in Table 2.

Figure 4. Leaf traits do not vary between cut and intact leaves or between leaves measured in the AM and PM groups with no significant effect on the estimated stomatal response parameters. Mean leaf mass per area (a), and fresh mass, dry mass ratio (b) are not different between treatments,

however there is a large among plant variation in these values. There is a significant difference in V_{cmax} (c) between AM and PM groups, however there is no difference between cut and intact groups. For R_{dark} (d) there are no significant differences either between AM and PM groups or cut and intact groups. Leaf structural properties have no significant relationship with g_0 (e-f) or g_1 (g-h) estimates within curves.

Figure 5. Model simulation results of rates of A and g_s given metrological data for an "average day" (06:00-18:30) during the period of measurement. Diurnal trends in (a) g_s and (b) A response for six different model runs conditioned on the mean g_1 and g_0 from the four treatments, the mean of all the data irrespective of treatment (population), and an dynamic model with the mean of the AM group used from 06:00-13:00 and the PM group used from 13:01-18:30. g_s rates respond strongly to the level of irradiance, temperature (e), VPD, and wind (f) which work in concert to produce a pronounced mid-day depression in g_s. Rates of A between model runs are different indicating stomatal limitation on A for the models with lower g_1 and g_0 parameter estimates. Total expected canopy (c) transpiration as a function of diurnal g_s and VPD, and (d) assimilation as a function of irradiance and leaf temperature. Error bars represent model runs using parameters ± 2 SE of their fitted means.

Figure 6. Observed experimental and predicted natural dynamics of light and rates of g_s measured on August 10, a typical day of measurement. Black and blue trend lines are the ambient PPFD and predicted rates of g_s based on metrological data and photosynthetic parameters (see methods). Note that the mid-day decline in g_s is due to an increase in VPD, rather than an effect of rates of A. Data in grey and red are the measurement PPFD and corresponding rates of g_s measured on intact leaves on the same day.

Table 1. Fixed effects components from the mixed effects models tested. Effects denoted with +0 are from the model where g_0 was $g_{0,population}$.

Model	Numerator df, Denominator df	F-value	Random effect SD	p-value	Contrast	Mean
g_0 ~ excision	2, 298	51.730	0.022	<0.001	g_0: Cut	0.037
					g_0: Intact	0.039
g_1 ~ excision	2, 289	71.011	0.840	<0.001	g_1: Cut	2.54
					g_1: Intact	2.76
g_1 ~ excision + 0	2, 300	102.177	0.917	<0.001	g_1: Cut	2.87
					g_1: Intact	3.15
g_0 ~ time	2, 298	20.151	0.016	<0.001	g_0: AM	0.052
					g_0: PM	0.023
g_1 ~ time	2, 298	126.615	0.607	<0.001	g_1: AM	2.10
					g_1: PM	3.26
g_1 ~ time + 0	4, 289	68.035	0.691	<0.001	g_1: AM	1.61
					g_1: PM	3.04

Table 2. Linear effect means and contrast estimates for the interactive effects of excision and time of day. Model denoted with +0 is the model where g_0 was $g_{0,population}$. Bolded values are significant with an alpha cutoff of 0.05. Sign (+/-) on the effect size indicates the direction of the comparison.

Model	Numerator df	F-value	Random effect SD	p-value	Effect	Mean	SE	Contrast	Effect size	t-value	p-value
g_0 ~ excision:time	4, 294	17.052	0.016	<0.001	AM-Cut	0.0556	0.00663	AM-Cut vs PM-Cut	-66%	3.941	**<0.001**
					AM-Intact	0.048	0.00665	AM-Cut vs AM-Intact	-14%	1.474	0.455
					PM-Cut	0.0189	0.00654	AM-Intact vs PM-Cut	-61%	-3.118	**0.011**
					PM-Intact	0.029	0.00658	AM-Cut vs PM-Intact	-48%	2.852	**0.024**
								PM-Cut vs PM-Intact	-53%	-2.038	0.176
								AM-Intact vs PM-Intact	-40%	2.033	0.178
g_1 ~ excision:time	4, 294	64.272	0.606	<0.001	AM-Cut	2.02	0.252	AM-Cut vs PM-Cut	49%	-2.731	**0.034**
					AM-Intact	2.18	0.252	AM-Cut vs AM-Intact	8%	-0.935	0.786
					PM-Cut	3.01	0.259	AM-Intact vs PM-Cut	37%	2.304	0.099
					PM-Intact	3.41	0.253	AM-Cut vs PM-Intact	69%	-3.883	**<0.001**
								PM-Cut vs PM-Intact	13%	-2.271	0.107
								AM-Intact vs PM-Intact	36%	-3.451	**0.004**
g_1 ~ excision:time + 0	4, 298	68.0350	0.727	<0.001	AM-Cut	1.52	0.23	AM-Cut vs PM-Cut	71%	-3.284	**0.006**
					AM-Intact	1.50	0.23	AM-Cut vs AM-Intact	-1.3%	0.135	0.999
					PM-Cut	2.60	0.238	AM-Intact vs PM-Cut	73%	3.335	**0.005**
					PM-Intact	3.25	0.231	AM-Cut vs PM-Intact	114%	-5.309	**<0.0001**
								PM-Cut vs PM-Intact	25%	-5.055	**<.0001**
								AM-Intact vs PM-Intact	117%	-5.364	**<.0001**

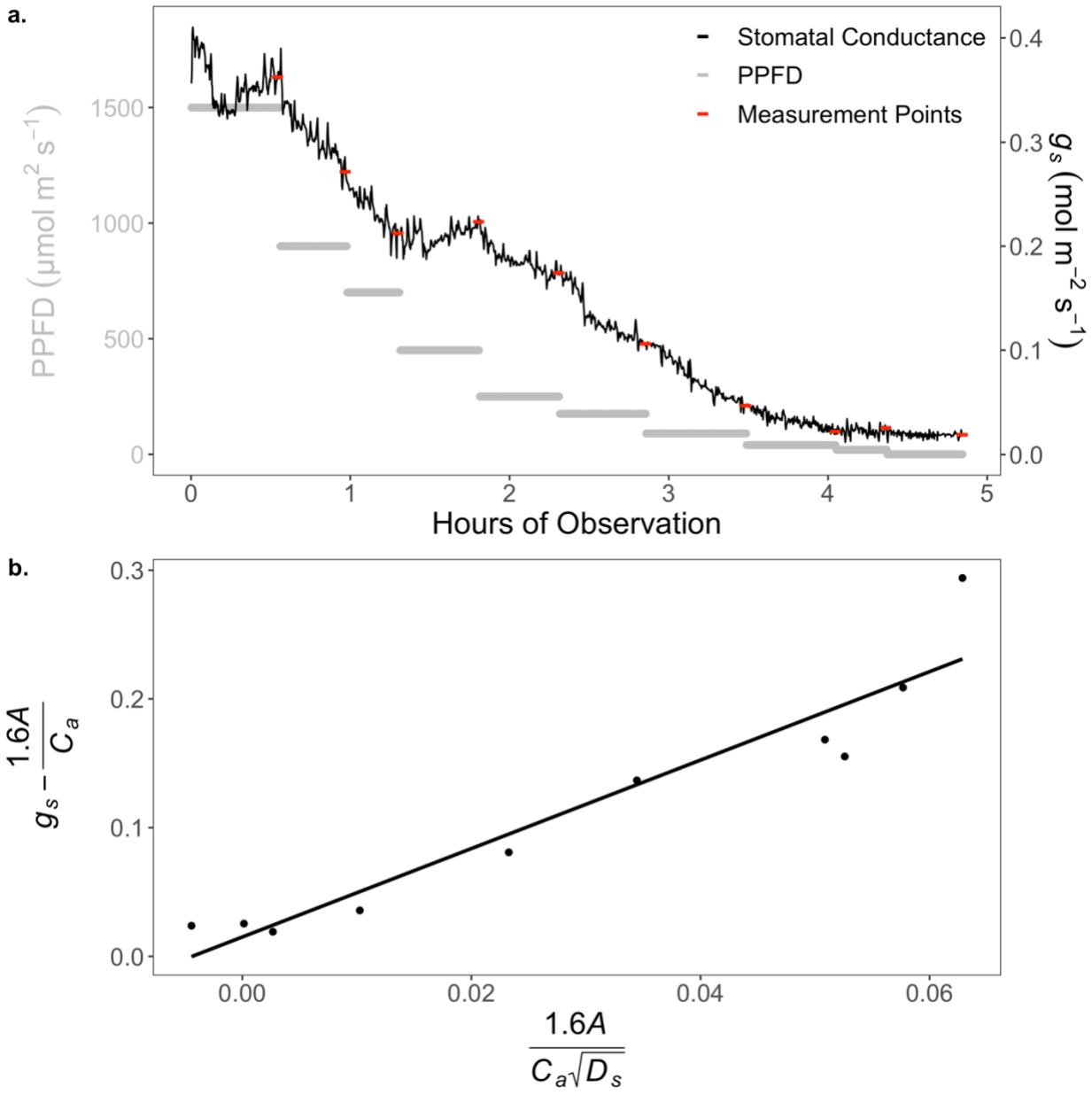

Figure 1. Overall format of the stomatal response curve approach in which irradiance is reduced in a stepwise manner, and rates of g_s decline in response. (a) Example of a curve in which rates of g_s reached steady state at each light level. Red points on the response curve correspond to the mean value for that irradiance level extracted for subsequent analysis. Even at steady state levels of g_s, there is still a great degree of observation-to-observation variation. (b) Standard visualization of the data from the curve conducted in (a). Plotting this way allows for a linear approximation of the g_1 and g_0 parameters, which are the slope and intercept respectively of the best fit line.

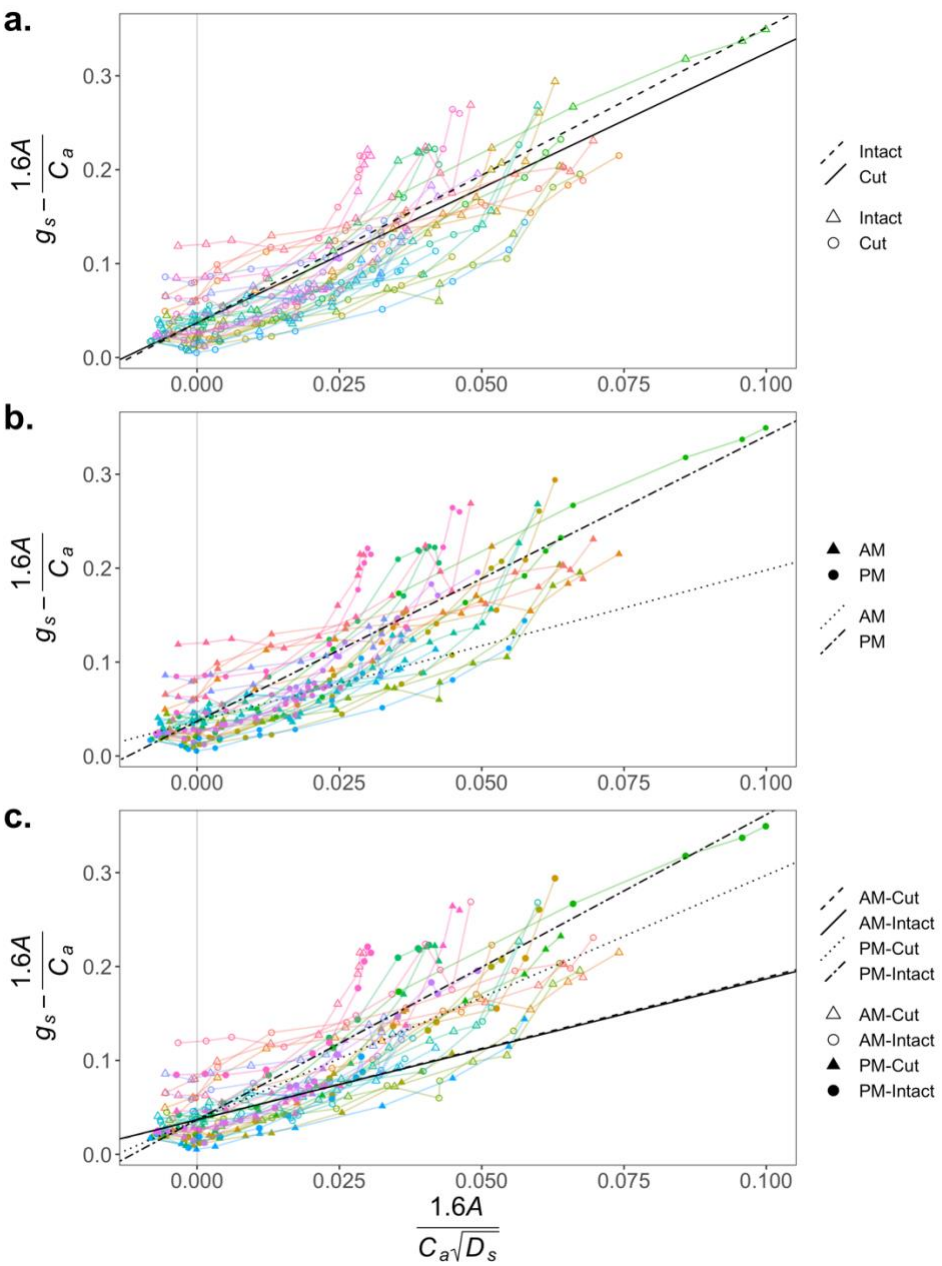

Figure 2. Effect of (a) excision and (b) time of day, and their interaction (c) on the fitted value of g_1 from the USO model, when g_0 is set to $g_{0,population}$ (0.037 mol m^2s^{-1}). Both excision and time of day produced a significant fixed effects relationship, with a 10% reduction in estimated g_1 for excised branches (a), and an 89% increase in g_1 from the AM treatment to the PM treatment (b). For the interaction (c) all contrast level differences are significant, except for the difference between cut and intact treatments during the AM time period. Notably, for the PM time period, predicted g_1 for the cut treatment was 25% less than the intact treatment, suggesting that the measurements are not comparable. Points connected by a colored line indicate that they were collected together as part of the same response curve. Points of the same color have the same random effects structure applied. Grey vertical line denotes the point of light compensation (A_n = 0)

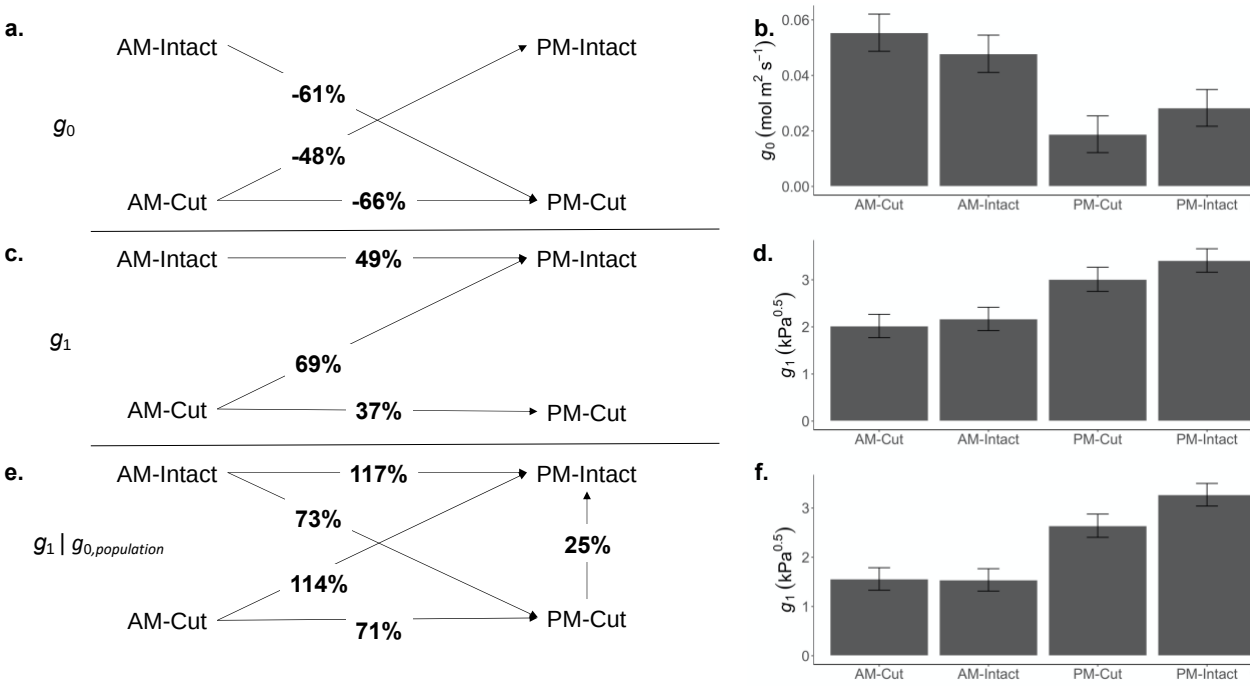

Figure 3. Comparisons of the interactive effects of excision and time of day on stomatal parameters. Percent difference between all six linear contrasts and absolute values and their error for (a-b) g_0 estimates, (c-d) g_1 estimates, and (e-f) g_1 estimates when g_0 is set to $g_{0,population}$. All differences reported in panels a, c, and e by percentage are significant. Error bars in panels b, d, and f are ± 2 SE, n=8. Full statistics and values for all effects are reported in Table 2.

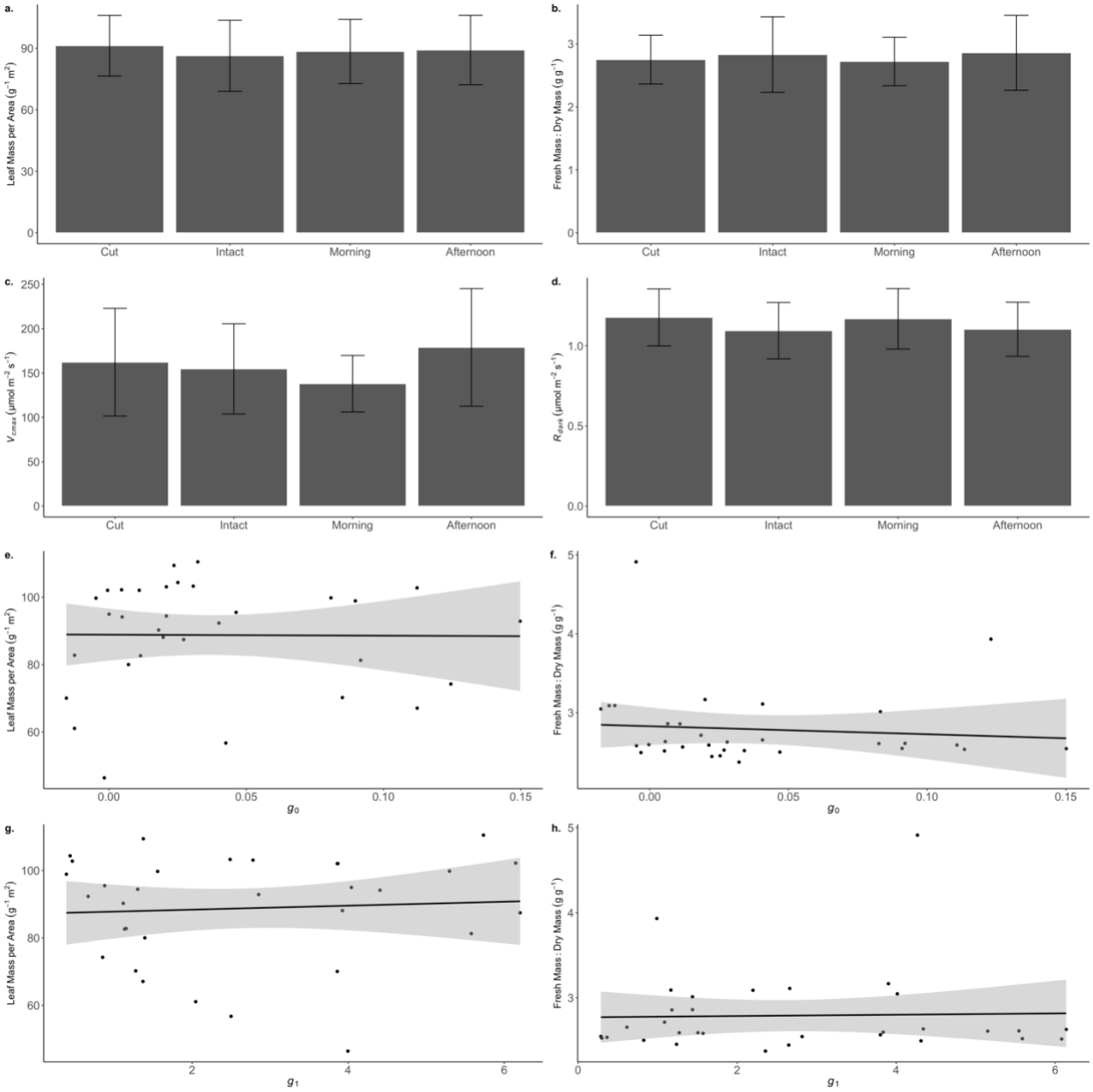

Figure 4. Leaf traits do not vary between cut and intact leaves or between leaves measured in the AM and PM groups with no significant effect on the estimated stomatal response parameters. Mean leaf mass per area (a), and fresh mass, dry mass ratio (b) are not different between treatments, however there is a large among plant variation in these values. There is a significant difference in V_{cmax} (c) between AM and PM groups, however there is no difference between cut and intact groups. For R_{dark} (d) there are no significant differences either between AM and PM groups or cut and intact groups. Leaf structural properties have no significant relationship with g_0 (e-f) or g_1 (g-h) estimates within curves.

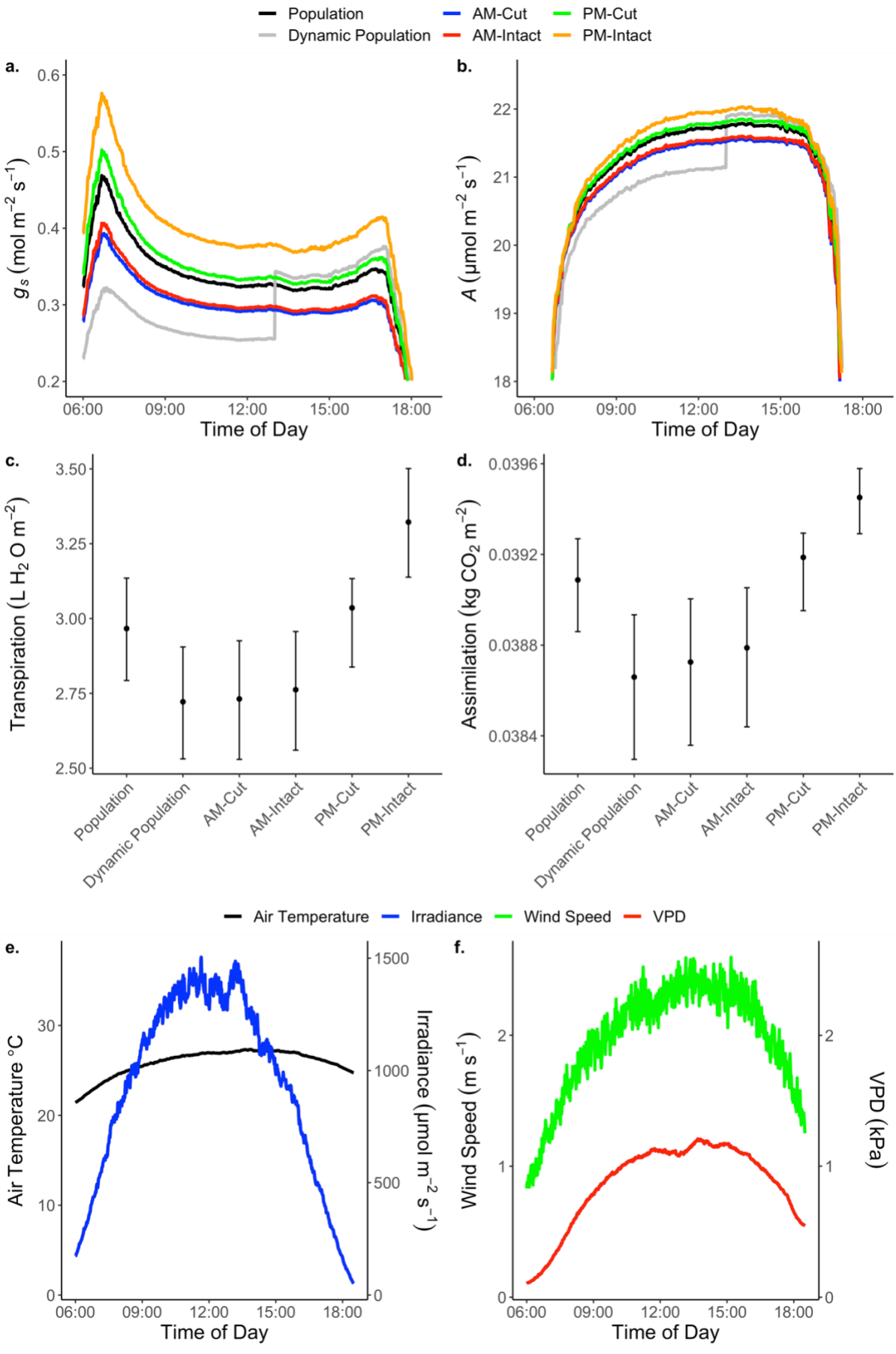
Population
Dynamic Population
AM-Cut
AM-Intact
PM-Cut
PM-Intact
a.
g_s (mol m^{-2} s^{-1})
Time of Day
b.
A (µmol m^{-2} s^{-1})
Time of Day
c.
Transpiration (L H_2O m^{-2})
d.
Assimilation (kg CO_2 m^{-2})
Air Temperature
Irradiance
Wind Speed
VPD
e.
Air Temperature °C
Irradiance (µmol m^{-2} s^{-1})
f.
Wind Speed (m s^{-1})
VPD (kPa)

Figure 5. Model simulation results of rates of A and g_s given metrological data for an "average day" (06:00-18:30) during the period of measurement. Diurnal trends in (a) g_s and (b) A response for six different model runs conditioned on the mean g_1 and g_0 from the four treatments, the mean of all the data irrespective of treatment (population), and an dynamic model with the mean of the AM group used from 06:00-13:00 and the PM group used from 13:01-18:30. g_s rates respond strongly to the level of irradiance, temperature (e), VPD, and wind (f) which work in concert to produce a pronounced mid-day depression in g_s. Rates of A between model runs are different indicating stomatal limitation on A for the models with lower g_1 and g_0 parameter estimates. Total expected canopy (c) transpiration as a function of diurnal g_s and VPD, and (d) assimilation as a function of irradiance and leaf temperature. Error bars represent model runs using parameters ± 2 SE of their fitted means.

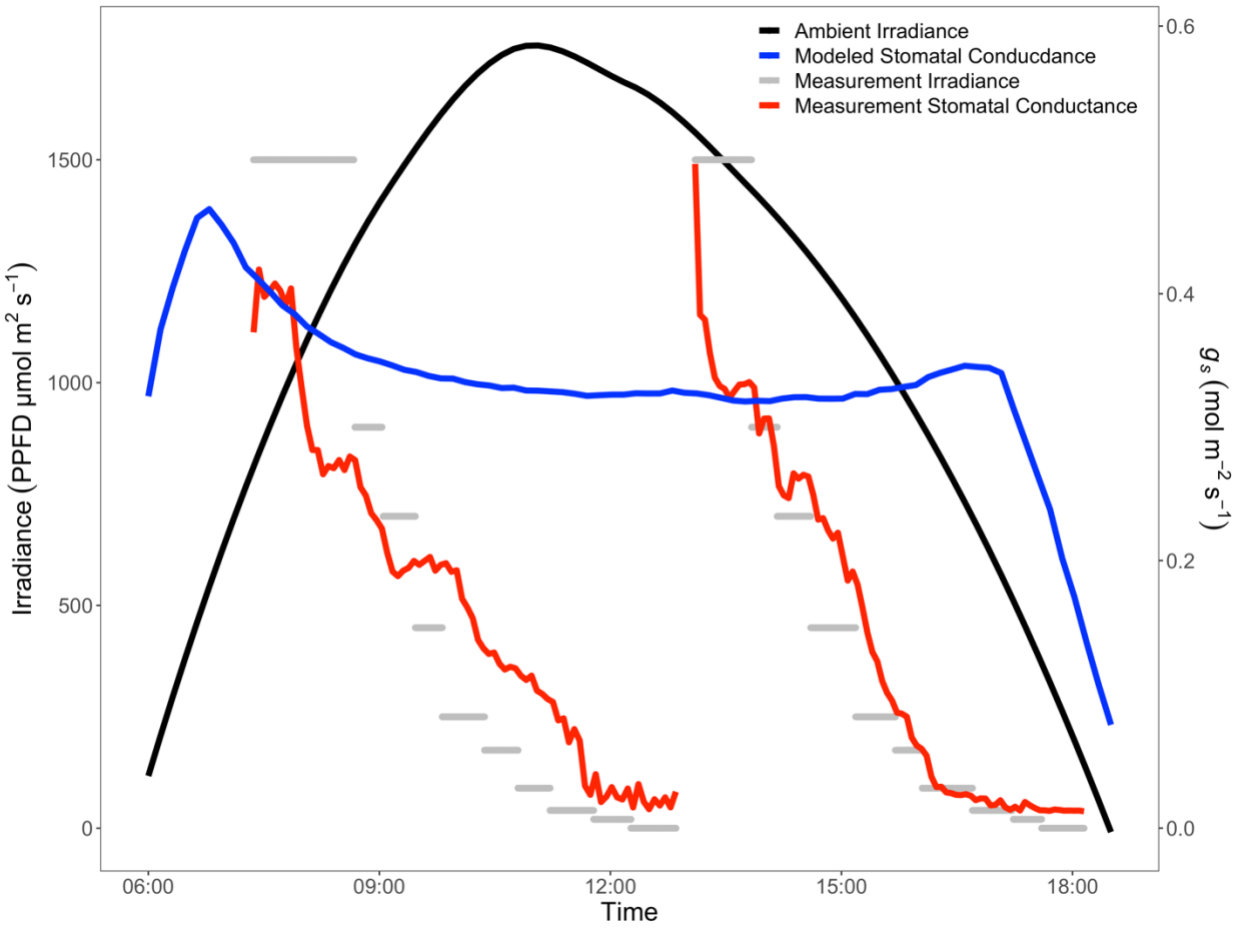

Figure 6. Observed experimental and predicted natural dynamics of light and rates of g_s measured on August 10, a typical day of measurement. Black and blue trend lines are the ambient PPFD and predicted rates of g_s based on metrological data and photosynthetic parameters (see methods). Note that the mid-day decline in g_s is due to an increase in VPD, rather than an effect of rates of *A.* Data in grey and red are the measurement PPFD and corresponding rates of g_s measured on intact leaves on the same day.

Supplemental Figures and Tables:

Table S1. Parameters used in the coupled photosynthesis, conductance, and energy balance models used for simulations in this study.

Parameter	Description	Default Value (units)	Source
R	Ideal gas constant	8.314 ($J\ mol^{-1}\ K^{-1}$)	-
O2	O_2 concentration in	210 (ppm)	-
TRef	Reference temperature for Kc, Ko, Rd, GammaStar Vcmax, Jmax	298.16 (K)	-
Patm	Atmospheric pressure	101 (kPa)	-
JmaxRef	Maximum electron transport rate	255.87 ($\mu mol\ m^{-2}\ s^{-1}$)	This study
JmaxHa	Energy of activation for Jmax	43540 ($J\ mol^{-1}$)	Bernacchi et al. (2001)*
JmaxHd	Energy of deactivation for Jmax	152040 ($J\ mol^{-1}$)	Bernacchi et al. (2001)*
JmaxS	Entropy term for Jmax	495 ($J\ mol^{-1}\ K^{-1}$)	Bernacchi et al. (2001)*
VcmaxRef	Maximum rate of Rubisco for carboxylation	158.43 ($\mu mol\ m^{-2}\ s^{-1}$)	This study
VcmaxHa	Energy of activation for Vcmax	65330 ($J\ mol^{-1}$)	Bernacchi et al. (2001)*
VcmaxHd	Energy of deactivation for Vcmax	149250 ($J\ mol^{-1}$)	Bernacchi et al. (2001)*
VcmaxS	Entropy term for Vcmax	485 ($J\ mol^{-1}\ K^{-1}$)	Bernacchi et al. (2001)*
RdRef	Respiration value at the reference temperature	1.13 ($\mu mol\ m^{-2}\ s^{-1}$)	This study
RdHa	Energy of activation for Rd	150650 ($J\ mol^{-1}$)	Bernacchi et al. (2001)*
KcRef	Michaelis-Menten constant of Rubisco for CO2 at the reference temperature	404.9 ($\mu mol\ mol^{-1}$)	Bernacchi et al. (2001)*
KcHa	Energy of activation for Kc	79430 ($J\ mol^{-1}$)	Bernacchi et al. (2001)*
KoRef	Michaelis-Menten constant of Rubisco for CO2 at the reference temperature	278.4 ($\mu mol\ mol^{-1}$)	Bernacchi et al. (2001)*
KoHa	Energy of activation for Ko	36380 ($J\ mol^{-1}$)	Bernacchi et al. (2001)*
GstarRef	CO2 compensation point in absence of respiration	42.75	Bernacchi et al. (2001)*
GstarHa	Enthalpy of activation for Gstar	37830 ($\mu mol\ mol^{-1}$)	Bernacchi et al. (2001)*
abso	Absorptance of the leaf in the photosynthetic active radiation wavelengths	0.85 (ratio)	-
aQY	Apparent quantum yield	0.425 (ratio)	-

Theta	Theta is the empirical curvature factor for the response of J to PFD	0.7 (ratio)	-

*Bernacchi, C.J., Singsaas, E.L., Pimentel, C., Portis Jr, A.R. and Long, S.P. (2001), Improved temperature response functions for models of Rubisco-limited photosynthesis. Plant, Cell & Environment, 24: 253-259. doi:10.1111/j.1365-3040.2001.00668.x

Table S2. Biochemical and functional properties estimated for each treatment group. Values in parentheses are the standard error of the mean

Property	AM	PM	Cut	Intact
LMA (g m^{-2})	88.44 (15.66)	89.14 (16.92)	91.23 (14.80)	86.35 (17.32)
FM/DM (g g^{-1})	2.72 (0.39)	2.85 (0.60)	2.75 (0.39)	2.83 (0.66)
V_{cmax} (µmol m^{-2} s^{-1})	138.97 (31.87)	178.90 (66.26)	162.19 (60.7)	154.68 (50.84)
R_{dark} (µmol m^{-2} s^{-1})	1.17 (0.19)	1.10 (0.17)	1.18 (0.18)	1.09 (0.18)

Table S3. Fixed effects components from the mixed effects model comparing photosynthetic parameters to leaf structural properties. None of the four models tested yielded a significant effect.

Model	Numerator df	Denominator df	F-value	p-value
g_0 ~ LMA	1	299	0.121	0.728
g_1 ~ LMA	1	299	1.100	0.295
g_0 ~ FM/DM	1	299	0.011	0.916
g_1 ~ FM/DM	1	299	0.057	0.812

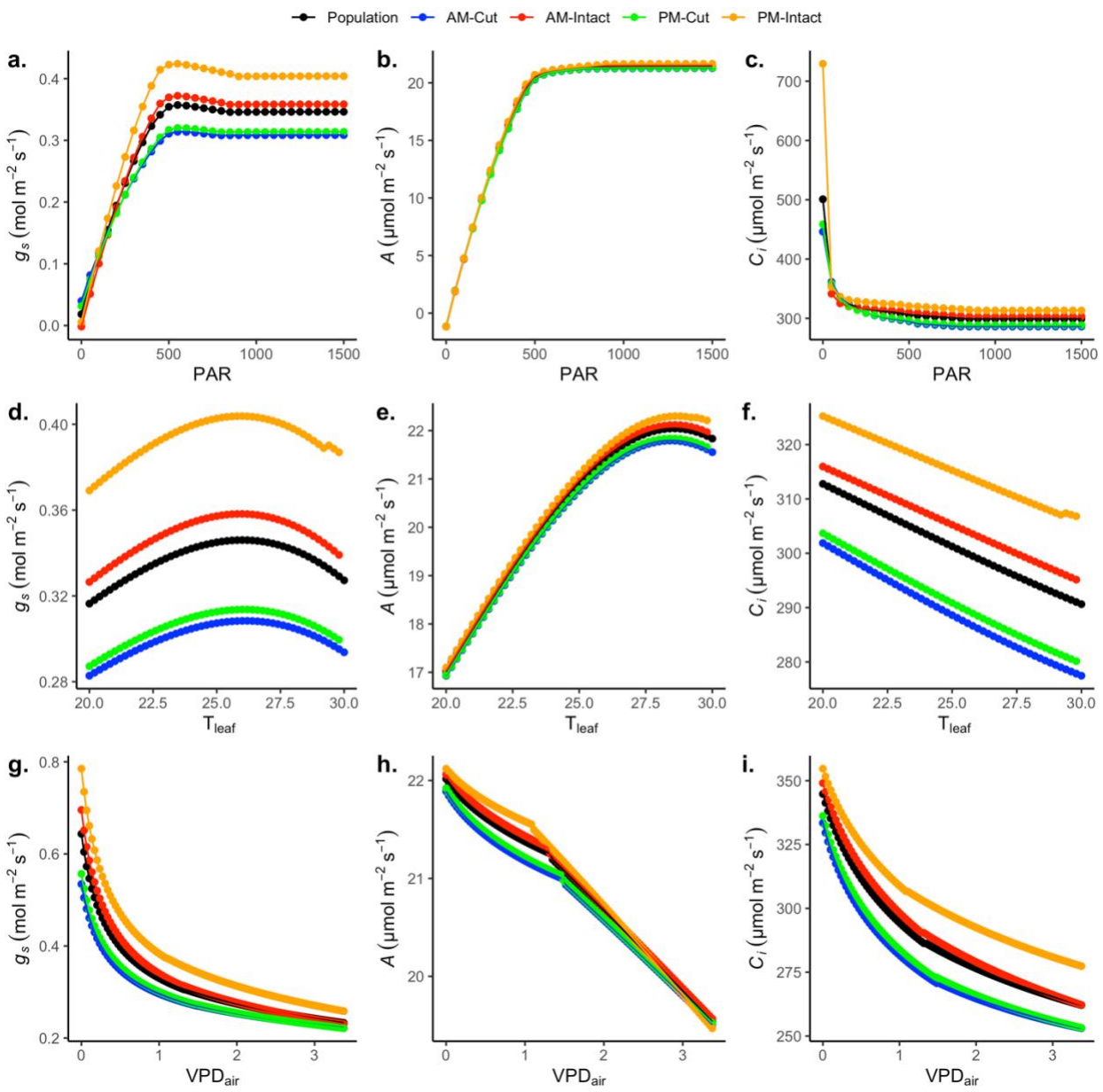

Figure S1. Diagnostic plots for g_s (a, d, g), A (b, e, h), and C_i (c, f, i) across an expected range of irradiance (a-c), leaf temperature (d-f) and VPD_{air} (g-i). For all simulations, T_{leaf} = 26, PAR= 1100, RH= 70%, wind= 2 ms^{-1}, and P_{atm}= 101.16 KPa, unless otherwise stipulated. g_0 and g_1 values were as follows, population: g_0 = 0.037, g_1 = 2.66; AM-cut: g_0 = 0.055, g_1 = 2.02; AM-intact: g_0 = 0.048, g_1 = 2.17; PM-cut: g_0 = 0.019, g_1 = 3.01; PM-intact: g_0 = 0.028, g_1 = 3.41; Shape of the responses were as expected and indicate that the model is performing well.

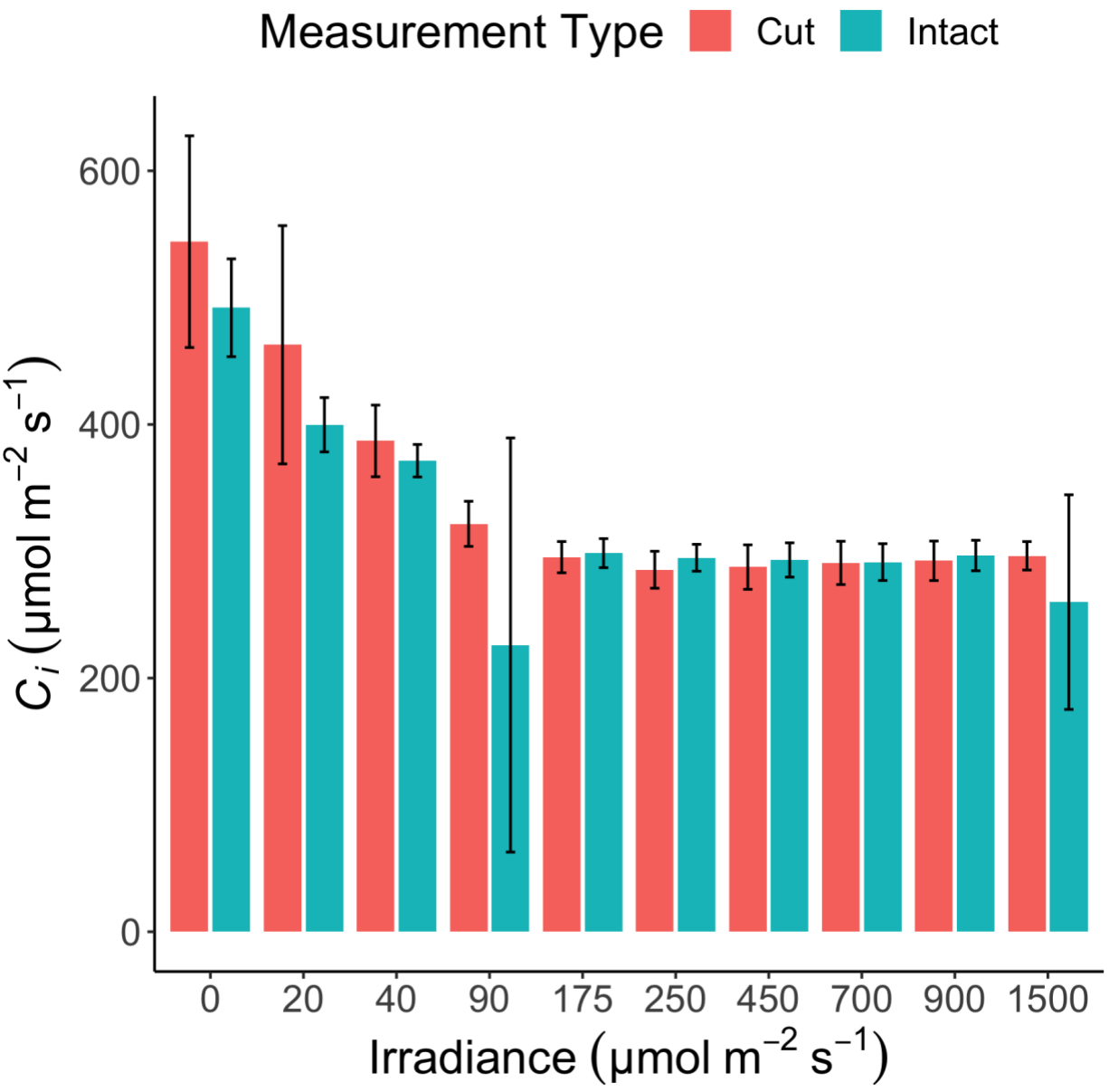

Figure S2. Comparison of values of C_i at each level of irradiance within a stomatal response curve. At each level there was no significant ($p < 0.05$) difference in C_i between pairs of cut and intact branches. Error bars represent ± 2 SE.